308 - - - Q200703120003

Scientific Notebook No. 391: Repository Design and Thermal-Mechanical Effects (RDTME) (02/18/2000 through 05/27/2005)

CNWRA
CONTROLLED
COPY 391

Doug Gute
210.522.2307

The Boorum & Pease® Quality Guarantee

The materials and craftsmanship that went into this product are of the finest quality. The pages are thread sewn, meaning they're bound to stay bound. The inks are moisture resistant and will not smear. And the uniform quality of the paper assures consistent rulings, excellent writing surface and erasability. If, at any time during normal use, this product does not perform to your expectations, we will replace it free of charge. Simply write to us:
Boorum & Pease Company
71 Clinton Road, Garden City, NY 11530
Attn: Marketing Services
Any correspondence should include the code number printed at the bottom of this page as well as the book title stamped at the bottom of the spine.

One Good Book Deserves Many Others.

Look for the complete line of Boorum & Pease® Columnar, Journal, and Record books. Custom-designed books also available by special order. For more information about our Customized Book Program, contact your office products dealer. See back cover for other books in this series.
Made in U.S.A.

Contents | Page

Title Page / Initial Entries	1
Identification of Engineered Barrier System Materials	2
Assumed Dimensions for the Drip Shield and Waste Package	19
Density Conversion for Titanium Drip Shield	22
Stress-Strain Curves for Titanium Drip Shield	23
Rock Block Geometry Derivation	26
Constitutive Model for the Rock Block	34
Initial Finite Element Analysis Objectives and Methodology	40
Preliminary Finite Element Analysis Results	48
Material Properties for Titanium Grade 5	58
Revised Material Properties for Titanium Grade 7	68
Bi-Linear Stress-Strain Curves for titanium Grades 5 and 7 and Alloy 22	69
Updated Drip Shield Dimensions	76
Emplacement Drift Cross-Section Illustrating the Relative Dimensions of the Drift Invert, Waste Package, and Drip Shield	78
Finite Element Analysis of Drip Shield Using New Design and Updated Material Properties	80
Summary of Finite Element Analysis Results of Rock Block and Drip Shield Impact (Scenario No. 1 and Updated Design)	85
Predicting the Maximum Drip Shield Displacement in Terms of the Rock Block Mass and Impact Velocity (Scenario No. 1 and Updated Design)	86
Summary of Finite Element Analysis of Rock Block and Drip Shield Impact (Scenario #2 on updated design)	89
Summary of Modal Analysis of Drip Shield	102

Repository Design and Thermal-Mechanical Effects (RDTME)

Doug Gute (Doug Gute)
Simon Hsiung
Darrell Dunn Luis Ibarra added 02/20/07
Doug Gute Asad Chowdhury
Added by D. Gute 1/21/02 Fernand Thomassy

This notebook documents the work being done to develop conceptual models including process-level WP analysis and rockfall study for upgrading SEISMO module to be included in the future version of the TPA code. See the Operations Plan for Repository Design and Thermal-Mechanical Effects (RDTME) for more details.

The qualifications required of the staff supporting this endeavor are as follows:

a) Computational Continuum Mechanics / Finite Element Analysis
b.) Material Science / Metallurgy
c) Rock Mechanics
d) Civil and Mechanical Engineering.
e) Geological Science and Engineering

Doug Gute 2/18/2000

Identification of Engineered Barrier System Materials

Drip Shield:

The material for the drip shield was identified as titanium grade 7. The drip shield will have an Alloy 22 "foot."

This information was obtained from the "Drip Shield Design" presentation given by Scott M. Bennett at the DOE/NRC Appendix 7 Meeting on EBS Testing on September 10, 1999.

From ASME B&PV Code, Section II, Part D - Properties, Table U, "Tensile Strength Values Su for Ferrous and Nonferrous Materials"

Nominal Composition - Ti-Pd
Product Form - Plate, sheet, strip
Specification No. - SB-265
Type / Grade - 7
Alloy Desig. / UNS No. - R52400
Class/Cond. / Temper - Annealed
Size / Thickness, in. - ...
Min. Tensile Strength - 50 ksi

Information potentially subject to copyright protection was redacted from this location.

The redacted material is from the information listed above.

From ASME B&PV Code, Section II, Part D - Properties, Table Y-1, "Yield Strength Values Sy for Ferrous and Nonferrous Materials"

Specification No. - SB-265
Type / Grade - 7
Alloy Desig. / UNS No. - R52400
Min. Yield Strength, ksi - 40

Information potentially subject to copyright protection was redacted from this location.

The redacted material is from the information listed on page 2.

From ASME B&PV Code, Section II, Part D - Properties, Table TE-5, "Thermal Expansion for Titanium Alloys"

Temperature (°F)	Coefficients for Titanium Alloy, Grades 1, 2, 3, 7, & 12
70	A = 4.4 B = 4.4 C = 0

Information potentially subject to copyright protection was redacted from this location.

The redacted material is from the information listed above.

A ≡ instantaneous coefficient of thermal expansion x 10^{-6} (in./in./°F)
B ≡ mean coefficient of thermal expansion x 10^{-6} (in./in./°F) in going from 70°F to indicated temperature
C ≡ linear thermal expansion (in./100ft) in going from 70°F to indicated temperature.

From 1998 ASME B&PV Code, Section II, Part D - Properties, Table TCD
"Nominal Coefficients of Thermal Conductivity (TC) and Thermal Diffusivity (TD)"

Unalloyed Titanium (Grades 1, 2, 3, 7, 16, + 17)

Information potentially subject to copyright protection was redacted from this location.

The redacted material is from the information listed above.

TC ≡ thermal conductivity, BTU/hr-ft-°F
TD ≡ thermal diffusivity, ft^2/hr : $TD = \frac{TC\ (BTU/hr\text{-}ft\text{-}°F)}{density\ (lb/ft^3) \times specific\ heat\ (BTU/lb\text{-}°F)}$

Note: • Values of thermal expansion and thermal diffusivity should be used with the understanding that there is an associated ± 10% uncertainty. This uncertainty results from compositional variations and variables associated with original data acquisition and analysis.

• The tabulated values of yield strength are those which the Committee believes are suitable for use in design calculations. At temperatures above room temperature, the yield strength values correspond to the yield strength trend curve adjusted to the minimum specified room temperature yield strength. The yield strength values do not correspond exactly to "minimum" as this term is applied to a statistical treatment of a homogeneous set of data.

• The tabulated values of tensile strength are those which the Committee believes are suitable for use in design calculations. At temperatures above room temperature, the values of tensile strength tend toward an average or expected value which may be as much as 10% above the tensile strength trend curve adjusted to the minimum specified room temperature tensile strength. The tensile strength values do not correspond exactly to "average" as this term is applied to a statistical treatment of a homogeneous set of data. Neither the ASME Material Specifications nor the rules of Sections I, III, or VIII require elevated temperature testing for tensile strengths of production material for use in Code components.

From 1998 ASME B&PV Code, Section II, Part D - Properties, Table TM-5
"Moduli of Elasticity E of Titanium and Zirconium for Given Temperatures"

Titanium / Grade 7 (UNS No.: R52400)

Information potentially subject to copyright protection was redacted from this location.

The redacted material is from the information listed above.

From 1998 ASME B&PV Code, Section II, Part D - Properties, Table NF-1
"Typical Mechanical Properties of Materials"

Unalloyed Titanium: Poisson's Ratio, $\nu = 0.32$
Modulus of Rigidity, $G = 6(10^6)$ psi

From 1998 ASME B&PV Code, Section II, Part D - Properties, Table NF-2
"Typical Physical Properties of Nonferrous Materials"

Unalloyed Titanium (UNS No.: R52400): density, $\rho \equiv 0.163$ lb/in^3
Approx. Melting Range $\simeq$ 3100°F
Specific Heat, $C_p \simeq$ 0.13 BTU/lb/°F @ 212°F

Doug [illegible] 2/22/2000

Waste Package (WP) Inner Barrier:

The material for the inner barrier of the WP was identified as being 316NG stainless steel, according to CRWMS - M&O Briefing entitled "Rock Fall Structural Analyses" given April 19, 1999 by Zekai Ceylan. According to Darrell Dunn of the CNWRA, 316NG (Nuclear Grade) properties can be approximated by 316L.
From the 1998 ASME B&PV Code, Section II, Part D - Properties, Table U, "Tensile Strength Values Su for Ferrous and Nonferrous Materials"

Nominal Composition - 16Cr - 12Ni - 2Mo
Product Form - Plate
Specification No. - SA-240
Type/Grade - 316L
Alloy Desig./UNS No. - S31603
Class/Cond./Temper - ...
Size/Thickness, in. - ...
Minimum Tensile Strength - 70 ksi

Information potentially subject to copyright protection was redacted from this location and the top of the next page..

The redacted material is from the information listed above

From 1998 ASME B&PV Code, Section II, Part D - Properties, Table Y-1,
"Yield Strength Values Sy for Ferrous and Nonferrous Materials."

Nominal Composition - 16Cr - 12Ni - 2Mo
Product Form - Plate
Specification No. - SA-240
Type/Grade - 316L
Alloy Desig./UNS No. - S31603
Class/Cond./Temper - ...
Size/Thickness, in. - ...
Minimum Yield Strength, - 25 ksi

Information potentially subject to copyright protection was redacted from this location.

The redacted material is from the information listed above.

From the 1998 ASME B&PV Code, Section II, Part D - Properties, Table TE-1, "Thermal Expansion for Ferrous Materials"

From Note (3) on p. 584, 16Cr-12Ni-2Mo belongs to Group 3 alloys.

Coefficients for Austenitic Stainless Steels (Group 3)

From the 1998 ASME B&PV Code, Section II, Part D - Properties, Table TCD, "Nominal Coefficients of Thermal Conductivity (TC) and Thermal Diffusivity (TD)"

From Note (11) on p. 606, 16Cr-12Ni-2Mo belongs to Material Group K

High Alloy Steels

Material Group K

Information potentially subject to copyright protection was redacted from this location.

The redacted material is from the information listed above.

From 1998 ASME B & PV Code, Section II, Part D - Properties, Table TM-1, "Moduli of Elasticity E of Ferrous Materials for Given Temperatures"

From Note (7) on p.606.2, 16Cr-12Ni and 16Cr-12Ni-2Mo-N are part of Material Group G. 16Cr-12Ni-2Mo is not part of anyother material group. Therefore, it is assumed that Material Group G represents 316L stainless steel.

Information potentially subject to copyright protection was redacted from this location.

The redacted material is from the information listed above.

From ASTM A240/A240M-98a, "Standard Specification for Heat-Resisting Chromium and Chromium-Nickel Stainless Steel Plate, Sheet, and Strip for Pressure Vessels."

UNS Designation - S31603 Minimum Elongation in 2in - 40%
Type/Grade - 316L

WP Outer Barrier:

The material for the outer barrier of the WP was identifie
being Alloy 22, according to the "Enhanced Design Alternatives
Findings: EDA II" presentation given by Rob Howard on Ap
CRWMS M&O Contractor, TRW Environmental Safety Syste

From 1998 ASME B & PV Code, Section II, Part D - Properties,
"Tensile Strength Values Su for Ferrous and Nonferrous Mater

Nominal Composition - 55Ni-21Cr-13.5Mo
Product Form - Plate, sheet, strip
Specification No. - SB-575
Type/Grade - ...
Alloy Designation/UNS No. - N06022
Class/Cond./Temper - Solution Annealed
Size/Thickness, in. - ...
Minimum Tensile Strength - 100 ksi

Information potentially subject to copyright protection was redacted from this location.

The redacted material is from the information listed above.

From 1998 ASME B&PV Code, Section II, Part D - Properties, Table Y-1
"Yield Strength Values Sy for Ferrous and Nonferrous Materials"

Nominal Composition - 55 Ni - 21 Cr - 13.5 Mo
Product Form - Plate, sheet, strip
Specification No. - SB-575
Type/Grade - ...
Alloy Designation/UNS No. - N06022
Class/Cond./Temper - solution annealed
Size/Thickness, in. - ...
Minimum Yield Strength - 45 ksi

Information potentially subject to copyright protection was redacted from this location.

The redacted material is from the information listed above.

According to the 1998 ASME B&PV Code, Section II, Part C - Specifications for Welding Rods, Electrodes, and Filler Metals, Table 3, "Base Metals for Test Assemblies," p. 263, ENiCrMo-4, 5, 7, 10, 13, 14, Low-Carbon-Nickel-Chromium-Molybdenum Alloy, SB575 is compatible with N10276, N06455, N06022, N06059, and N06686.

Because Table TE-4 of the 1998 ASME B&PV Code, Section II, Part D - Properties does not have thermal expansion data for N06022 specifically, N10276 and N06455 may be adequate approximations. So, from the 1998 ASME B&PV Code, Section II, Part D - Properties, Table TE-4, "Thermal Expansion for Nickel Alloys."

Coefficients for N06455 Coefficients for N10276

Information potentially subject to copyright protection was redacted from this location.

The redacted material is from the information listed above.

Because N06022 is not explicitly included in Table TCD of the 1998 ASME B&PV Code, Section II, Part D - Properties, "Nominal Coefficients of Thermal Conductivity (TC) and Thermal Diffusivity (TD)," the values for N06455 and N10276 are assumed to provide good approximations (see the bottom of p. 12 of this scientific notebook).

N06455 N10276

Information potentially subject to copyright protection was redacted from this location.

The redacted material is from the information listed above.

*TBD - To Be Determined

DA 2/24/2000

Because N06022 is not explicitly included in Table TM-4 of the 1998 ASME B&PV Code, Section II, Part D - Properties, "Moduli of Elasticity E of High Nickel Alloys for Given Temperatures," the values for N06455 and N10276 are assumed to provide good approximations (see the bottom of p. 12 of this scientific notebook).

N06455 N10276

Information potentially subject to copyright protection was redacted from this location.

The redacted material is from the information listed above.

From ASTM Designation: B 575-98, "Standard Specification for Low-Carbon Nickel-Molybdenum-Chromium, Low-Carbon Nickel-Chromium-Molybdenum, Low-Carbon Nickel-Chromium-Molybdenum-Copper, Low-Carbon Nickel-Chromium-Molybdenum-Tantalum, and Low-Carbon Nickel-Chromium-Molybdenum-Tungsten Alloy Plate, Sheet, and Strip"

Information potentially subject to copyright protection was redacted from this location.

The redacted material is from the information listed above.

Based on updated information obtained from Gustavo Castigliano, it was determined that the material properties for stainless steel 316L would not be representative of the material used for the inner barrier of the waste package. Instead, stainless steel 316LN should be used. In the event that this material information is not readily available, then the material properties for stainless steel 316 should be used.

From the ASME B&PV Code, Section II, Part D-Properties, Table U, "Tensile Strength Values Su for Ferrous and Nonferrous Materials"

For 316LN:

Nominal Composition - 16Cr-12Ni-2MO-N
Product Form - Plate
Specification No. - SA240
Type/Grade - 316LN
Alloy Designation/UNS No. - S31653
Class/Cond./Temper - ...
Size/Thickness, in. - ...
Minimum ~~Yield~~ Tensile Strength - 75 ksi

Information potentially subject to copyright protection was redacted from this location.

The redacted material is from the information listed above.

From the ASME B&PV Code, Section II, Part D-Properties, Table Y-1, "Yield Strength Values Sy for Ferrous and Nonferrous Materials"

Nominal Composition - 16Cr-12Ni-2Mo-N
Product Form - Plate
Specification No. - SA240
Type/Grade - 316LN
Alloy Designation/UNS No. - S31653
Class/Cond./Temper - ...
Size/Thickness, in. - ...
Minimum Yield Strength - 30 ksi

Information potentially subject to copyright protection was redacted from this location.

The redacted material is from the information listed above.

From the 1998 ASME B&PV Code, Section II, Part D-Properties, Table TE-1, "Thermal Expansion for Ferrous Materials"

From Note (3) on page 584, 16Cr-12Ni-2Mo-N belongs to Group 3 alloys. As a result, the thermal expansion values correspond with those having a Nominal Composition of 16Cr-12Ni-2Mo. See page 8 of this scientific notebook.

The thermal conductivity for 16Cr-12Ni-2Mo-N is not explicitly provided in the 1998 ASME B&PV Code, Section II, Part D - Properties, Table TCD, "Nominal Coefficients of Thermal Conductivity (TC) and Thermal Diffusivity (TD)." As a result, it will be assumed that the values for stainless steel 316 (16Cr-12Ni-2Mo) apply. See page 9 of this scientific notebook.

From 1998 ASME B&PV Code, Section II, Part D - Properties, Table TM-1, "Moduli of Elasticity E of Ferrous Materials for Given Temperatures"

From Note (7) on page 606.2, 16Cr-12Ni-2Mo-N is part of material group G. See page 10 of this scientific notebook.

From ASTM A240/A240M-98a, "Standard Specification for Heat-Resisting Chromium and Chromium-Nickel Stainless Steel Plate, Sheet, and Strip for Pressure Vessels."

UNS Designation - S31653
Type - 316LN
Minimum Tensile Strength - 75 ksi
Minimum Yield Strength - 30 ksi
Min. Elongation in 2in., % - 40.0%

Doug Gute 2/24/2000

Assumed Dimensions for the Drip Shield and Waste Package

The following schematic of the Engineered Barrier System Components was obtained from the presentation by Ms. Suzanne Mellington, U.S. Department of Energy, Office of Project Execution entitled "Status of Scientific Testing and Repository Design." This presentation was given at the Waste Management Symposium 2000.

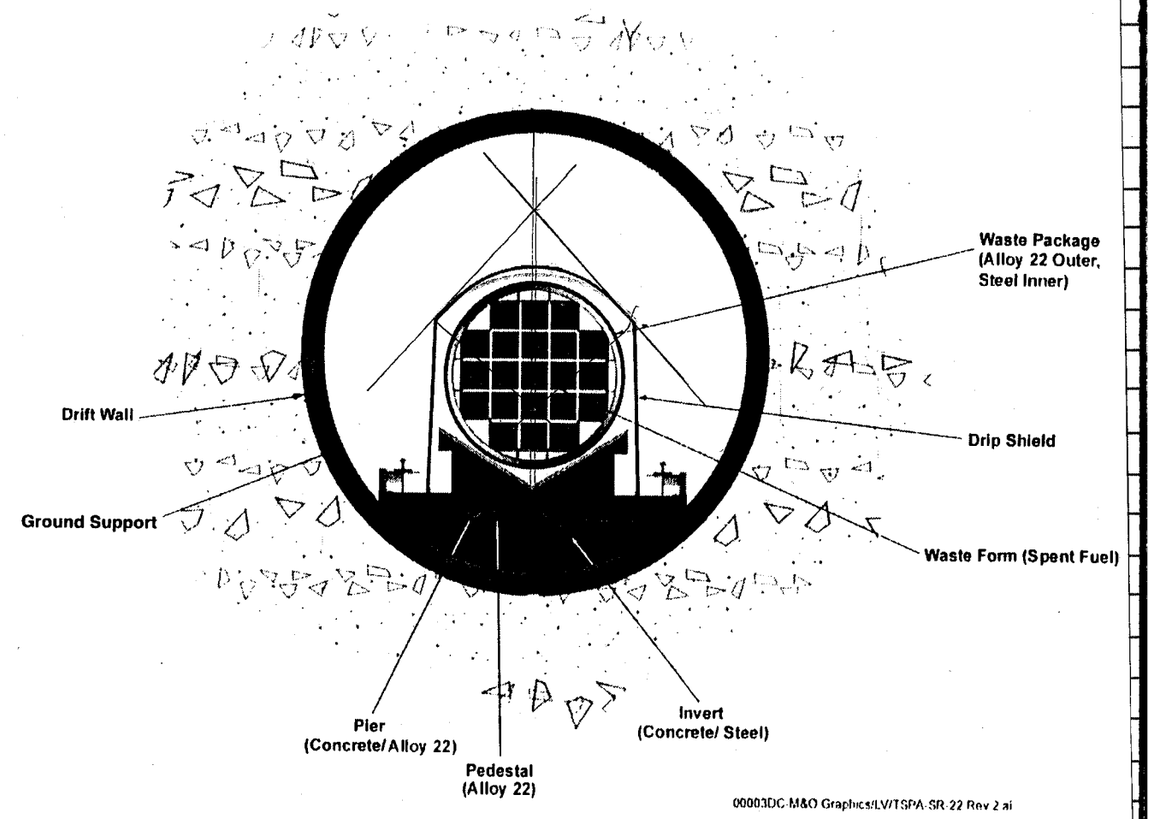

YMP Yucca Mountain Project/Preliminary Predecisional Draft Materials

The schematic on page 19 of this scientific notebook will be used to estimate the dimensions of the drip shield. For the 21 PWR Fuel Basket that is depicted in the schematic, the width and height for any given SNF assembly tube is 0.2335m (see the VA design details). In addition, the inner diameter of the inner barrier is 1.389m. These observations, when applied to the schematic on page 19, lead to a drawing scale of 1.39 m/in. This scale is subsequently used to extract the following dimensions for the drip shield. Note that the drip shield is 0.020m thick and the dimensions below correspond to the midsurface.

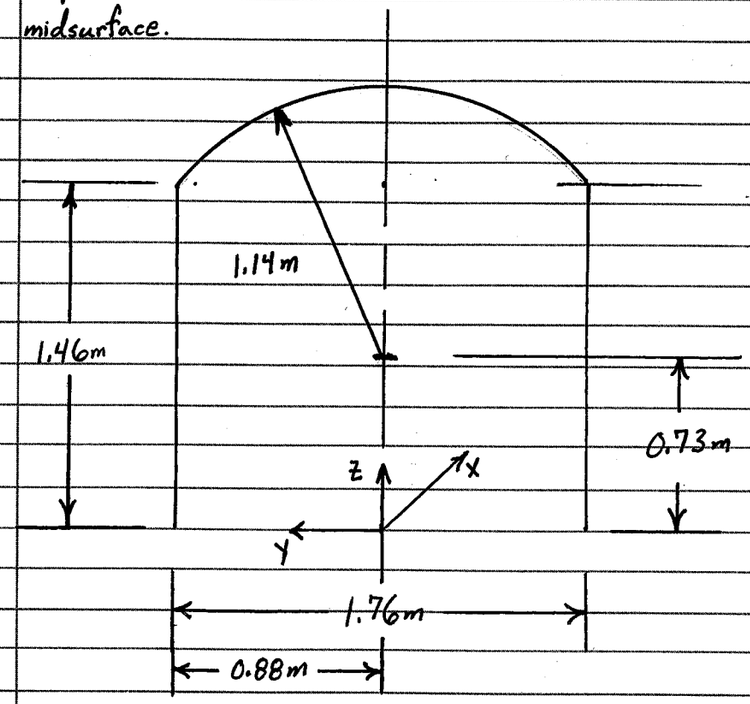

The length of the drip shield will be assumed to be 5.5m.

The dimensions for the inner and outer barries of the waste package are compatible with the 21 PWR Fuel Basket shown on page 19 of this scientific notebook. The inner radius of the inner barrier is consistent with the VA waste package design. The thicknesses of the inner and outer barriers, however, have been updated to conform to the proposed EDA II waste package dimensions. Specifically,

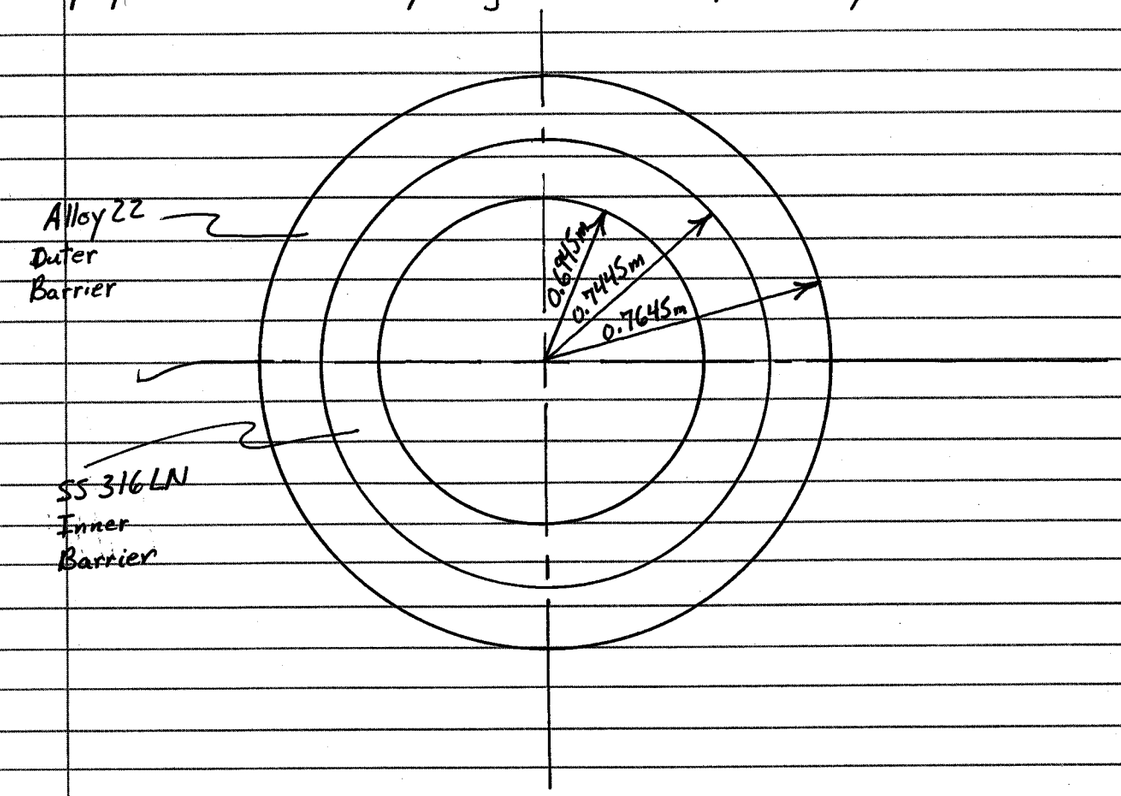

Note: Sketch Not To Scale!

Craig Stirte 3/2/2000

Density Conversion for Titanium Drip Shield

From page 6 of this scientific notebook:

$$\rho = 0.163 \frac{lb}{in^3} \quad ; \text{ weight density}$$

Because the rockfall simulation is being performed using SI units, the density must be converted to kg/m^3

$$\rho = \left(0.163 \frac{lb}{in^3}\right)\left(\frac{1}{0.0254}\frac{in}{m}\right)^3\left(4.448222 \frac{N}{lb}\right)$$
$$= 44245.8872 \frac{N}{m^3}$$

Convert to mass density,

$$\rho = \frac{(44245.8872\ N/m^3)}{(9.806650\ m/s^2)}$$
$$= 4511.8249 \frac{kg}{m^3}$$

$$\therefore \rho = 4512 \frac{kg}{m^3}$$

Doug Ende 3/3/2000

Stress-Strain Curves for Titanium Drip Shield

NOTE: It was found that the yield stress values for Ti-7 as presented in the 1998 ASME B&PV Code may be in error. See "Revised Material Properties for Titanium Grade 7" on p. 68 of this notebook. Doug Ende 6/28/2000

"Engineering" Stress-Strain Curve
Titanium/Grade 7

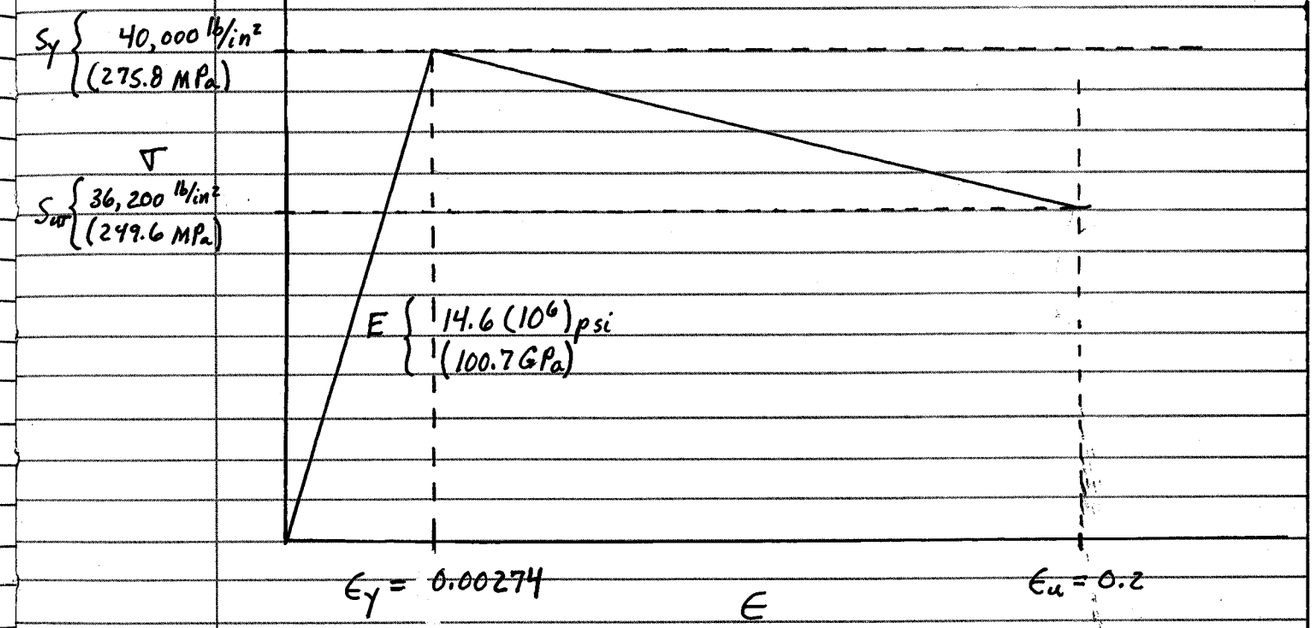

It is assumed that the drip shield will have a temperature of 300°F (150°C) when placed into service within the emplacement drift. As a result:

Tensile Strength, S_{UT} = 36.2 ksi (249.6 MPa); from p. 2.
Yield Stress, S_y = 40.0 ksi (275.8 MPa); from p. 3
Modulus of Elasticity, E = 14.6 (10^6) psi (100.7 GPa); from p. 5
Min. Elongation in 2 in. or 50 mm, ϵ_u = 20% (0.200); from ASTM B265-98
Yield Strain, $\epsilon_y = \frac{S_y}{E} = \frac{(40{,}000\ psi)}{(14{,}600{,}000\ psi)} = 0.00274$

When defining the material behavior in the plastic range ABAQUS requires that the stress-strain be defined as "true stress" and logarithmic plastic strain. The conversion equations from the "nominal," i.e. "engineering," values to the "true" and "logarithmic" forms is as follows:

$$\sigma_{true} = \sigma_{nom}(1+\epsilon_{nom})$$

$$\epsilon_{ln}^{pl} = \ln(1+\epsilon_{nom}) - \frac{\sigma_{true}}{E}$$

From the ABAQUS/Explicit User's Manual, Volume I, Version 5.8, page 10.1.1-3.

At the yield point,

$$\sigma_{true} = 276\,MPa\,(1+0.00274)$$
$$= 277\,MPa$$
$$\epsilon_{ln}^{pl} = 0.00$$

At the ultimate strength point,

$$\sigma_{true} = 250\,MPa\,(1+0.20)$$
$$= 300\,MPa$$
$$\epsilon_{ln}^{pl} = \ln(1+0.20) - \frac{300\,MPa}{100{,}700\,MPa}$$
$$= 0.1793$$

"True" Stress - Log Strain
Titanium/Grade 7

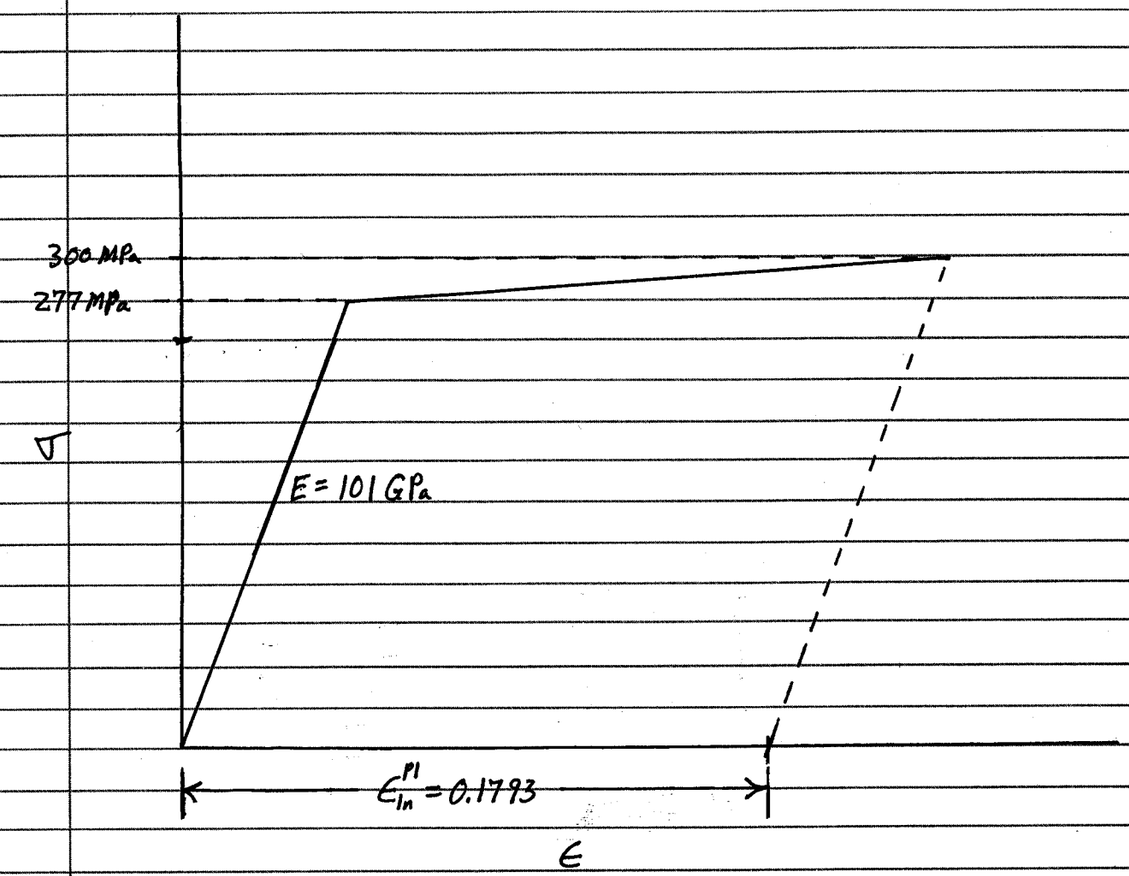

Doug [illegible] 3/8/2000

Rock Block Geometry Derivation

To: Doug Gute
From: Amit Ghosh
Date: March 29, 2000
CC: Simon Hsiung, Asad Chowdhury
Subject: Estimation of largest kinematically displaceable rock block in an emplacement drift

I have carried out the analysis to estimate the size of the largest rock block that can fall from a roof of an emplacement drift at the potential repository at Yucca Mountain. The analysis follows the suggested methodology of Hoek and Brown (1980). The assumption is that the failure is structurally controlled and the block separates from the surrounding rock mass under gravity load by at least three intersecting structural discontinuities (here, joints).

The joint set data used in the analysis are as follows (Civilian Radioactive Waste Management System Management and Operating Contractor, 1997):

Table 1. Joint set parameters used in the analysis

Joint Set	Dip (degree)	Dip Direction (degree)	Joint Spacing (m)	Cohesion (tonnes/m^2)	Friction Angle (degree)	Rock Density (tonnes/m^3)	Water Pressure (tonnes/m^2)
A	78	262	1	0	30	2.7	0
B	82	132	1	0	30	2.7	0
C	84	353	1	0	30	2.7	0

The dip direction of an emplacement drift is taken as 105°. The diameter of the drift is 5.5 m. For simplifying the calculation, the drift is assumed as square cross-section with each side 5.5 m in length.

For a rock block (i.e., a wedge) to fall under gravity without any sliding on at least one of the joint planes, a vertical line drawn through the apex of the wedge must pass through the base of the wedge. Figure 1 proves that.

Three joint planes are represented on the stereoplot by their great circles, marked *A*, *B*, *C* in Figure 1. The strike lines of these planes are marked as *a*, *b*, and *c*, respectively. The traces of the vertical planes through the center of the net and the great circle intersections are marked by *ab*, *ac*, and *bc*. The directions of the strike lines correspond to the traces of the joint planes *A*, *B*, and *C* on the horizontal roof of the drift.

In the plan view, the apex of the wedge is defined by the intersection points of lines *ab*, *bc*, and *ac*, projected from the corners of the triangular wedge base. The height *h* of the apex of the wedge above the horizontal drift roof has been determined by taking a section through the wedge apex and normal

to the tunnel axis. The apparent dips of the planes *C* and *A* are 72° and 84°, respectively. These angles were measured from the stereographic projection.

The base area of the wedge Δ is:

$$\Delta = \sqrt{s(s-la)(s-lb)(s-lc)} = 10.36 \text{ m}^2$$

where,

la = length of side a = 4.98 m
lb = length of side b = 6.27 m
lc = length of side c = 4.17 m

$$s = \frac{la + lb + lc}{2} = 7.71 \text{ m}$$

The volume of the wedge = ⅓ $h\,\Delta$ = 30 m^3, which translates to a block with weight of 81 tonnes.

This analysis estimates the largest block that can be kinematically dislodge from the roof of the emplacement drift. This should be the first starting point of preliminary study of rock fall in a drift/tunnel excavated in a jointed rock mass. As Table 1 shows, this largest rock block will have several fractures/joints that either will reduce the size of the ultimate block that may dislodge from the roof or break during an impact with another surface and, thereby, absorbing significant part of the kinetic energy of the block. That should be the next step of the analysis.

References:

Civilian Radioactive Waste Management System Management and Operating Contractor. Yucca Mountain Site Geotechnical Report, Volume I. B00000000-01717-5705-00043 Rev 01. North Las Vegas, NV: TRW Environmental Safety Systems, Inc., 1997.

Hoek, E. and E.T. Brown. Underground Excavations in Rock. London, UK: The Institution of Mining and Metallurgy, 1980.

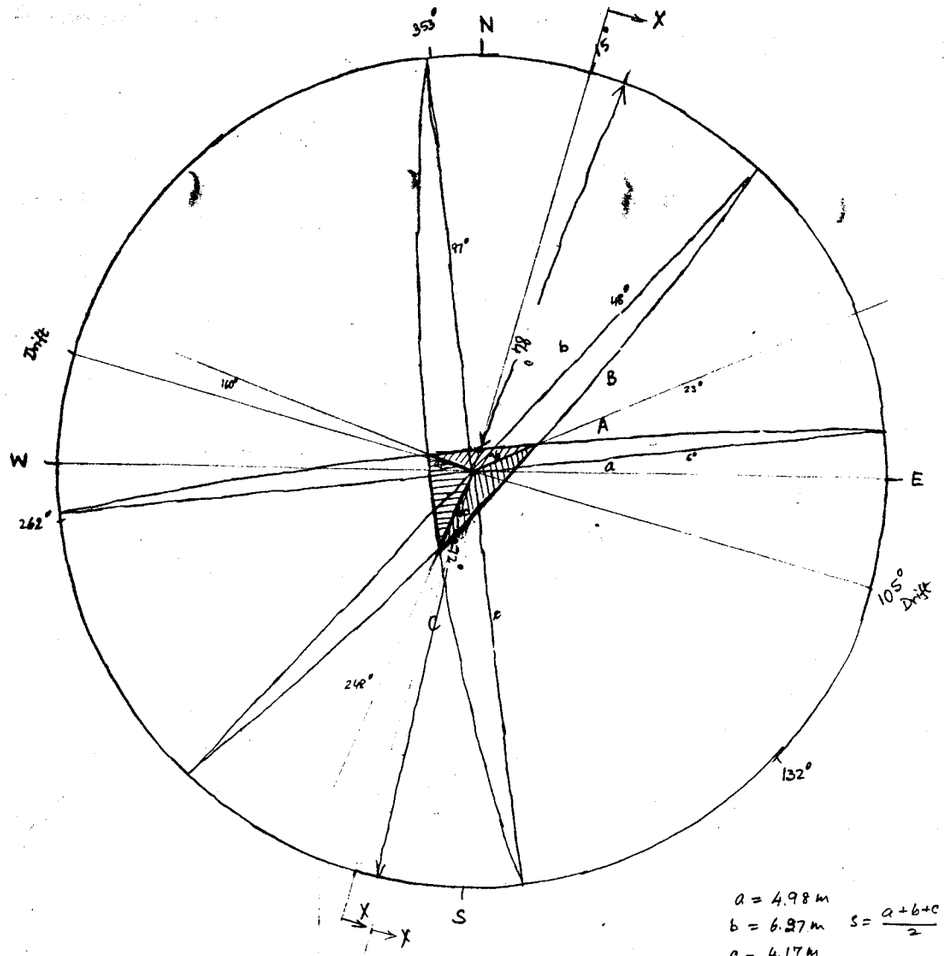

$a = 4.98\,m$
$b = 6.27\,m$
$c = 4.17\,m$

$s = \frac{a+b+c}{2} = 7.71\,m$

$\Delta = \sqrt{s(s-a)(s-b)(s-c)} = 10.36\,m^2$

$\text{Volume} = \frac{1}{3} h \Delta = \frac{1}{3} \times 8.7 \times 10.36 = 30\,m^3$

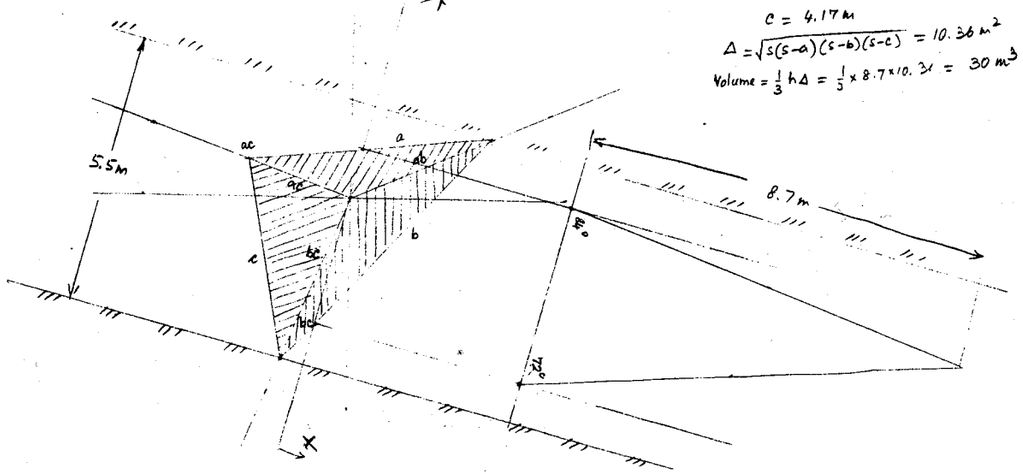

$a_o = 4.98\,m$ $\quad ac_o = 2.17\,m$ $\quad ac_o' = [(ac)^2 + (h)^2]^{1/2} = 8.97\,m$

$b_o = 6.27\,m$ $\quad ab_o = 3.11\,m$ $\quad ab_o' = [(ab)^2 + (h)^2]^{1/2} = 9.24\,m$

$c_o = 4.17\,m$ $\quad bc_o = 3.61\,m$ $\quad bc_o' = [(bc)^2 + (h)^2]^{1/2} = 9.42\,m$

$h_o = 8.7\,m$

This "white out" situation was noted during an audit 6/21/2000. PI was told not to ever use white out!

[illegible] 6/21/2000

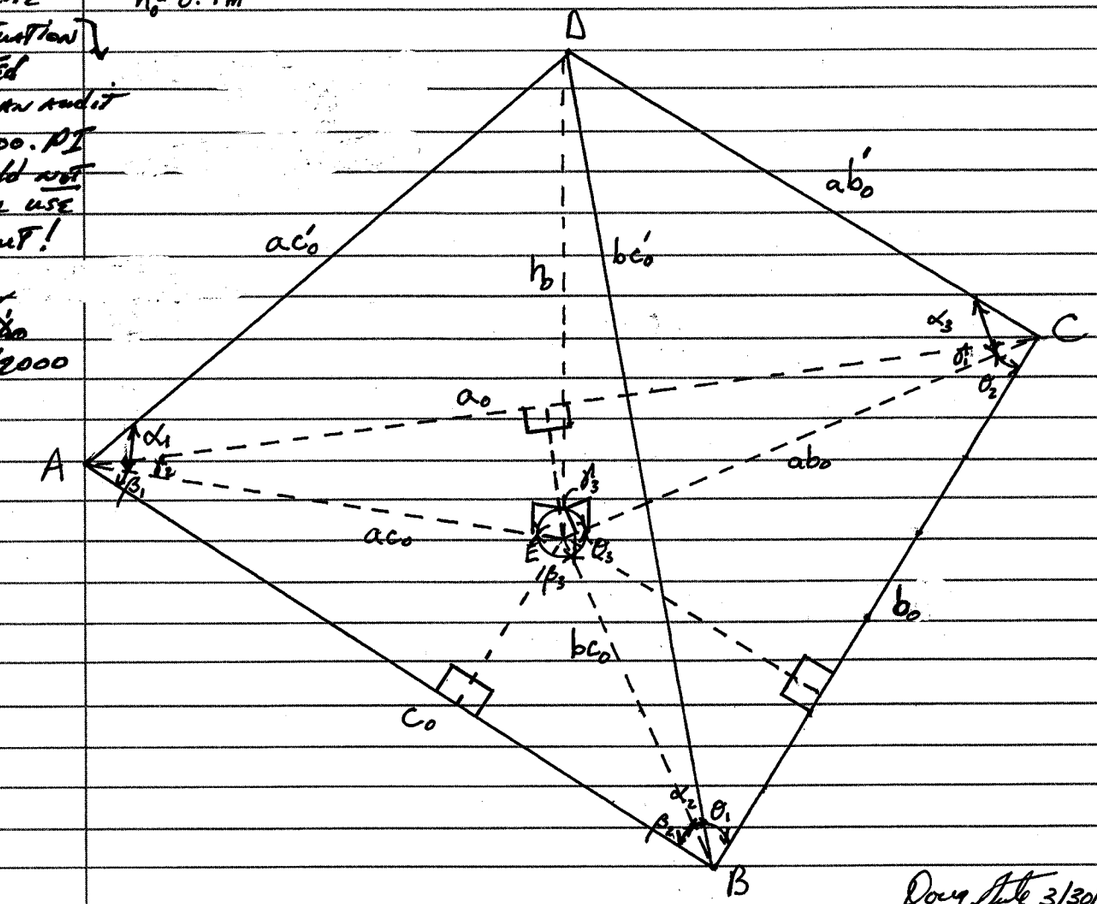

Doug [illegible] 3/30/2000

March 31, 2000:

After meeting with Asad Chowdhury, Simon Hsiung, and Amit Ghosh it was decided to scale the rock block dimensions used above to reduce the weight of the rock to 20 tonnes (20,000 kg).

To accomplish this task all of the dimensions of the tetrahedral rock block will be recast in terms of the height, h, defined above. In addition, the angles α_i, β_i, θ_i, and γ_i $(i = 1, 2, 3)$ will be kept constant.

EJ 6/21/2000

Doug [illegible] 3/31/2000

DJ 6/21/2000

In terms of the initial ~~conditions~~ dimensions, $\alpha_i, \beta_i, \theta_i$, and γ_i are

$$\alpha_1 = \tan^{-1}\left(\frac{h_o}{ac_o}\right) = \tan^{-1}\left(\frac{8.7}{2.17}\right) = 76.0^\circ$$

$$\alpha_2 = \tan^{-1}\left(\frac{h_o}{bc_o}\right) = \tan^{-1}\left(\frac{8.7}{3.61}\right) = 67.5^\circ$$

$$\alpha_3 = \tan^{-1}\left(\frac{h_o}{ab_o}\right) = \tan^{-1}\left(\frac{8.7}{3.11}\right) = 70.3^\circ$$

$$\beta_1 = \cos^{-1}\left[\frac{(ac_o)^2 + (c_o)^2 - (bc_o)^2}{(2)(ac_o)(c_o)}\right] \quad ; \text{ law of cosines}$$
$$= 59.9^\circ$$

$$\beta_2 = \cos^{-1}\left[\frac{(bc_o)^2 + (c_o)^2 - (ac_o)^2}{(2)(bc_o)(c_o)}\right] = 31.4^\circ$$

$$\beta_3 = \cos^{-1}\left[\frac{(ac_o)^2 + (bc_o)^2 - (c_o)^2}{(2)(bc_o)(c_o)}\right] = 88.7^\circ$$

Note: $\beta_1 + \beta_2 + \beta_3 = 180^\circ$

$$\theta_1 = \cos^{-1}\left[\frac{(b_o)^2 + (bc_o)^2 - (ab_o)^2}{(2)(b_o)(bc_o)}\right] = 19.5^\circ$$

$$\theta_2 = \cos^{-1}\left[\frac{(b_o)^2 + (ab_o)^2 - (bc_o)^2}{(2)(b_o)(ab_o)}\right] = 22.8^\circ$$

$$\theta_3 = \cos^{-1}\left[\frac{(ab_o)^2 + (bc_o)^2 - (b_o)^2}{(2)(ab_o)(bc_o)}\right] = 137.7^\circ$$

Note: $\theta_1 + \theta_2 + \theta_3 = 180^\circ$

$$\gamma_1 = \cos^{-1}\left[\frac{(a_o)^2 + (ab_o)^2 - (ac_o)^2}{(2)(a_o)(ab_o)}\right] = 16.1^\circ$$

$$\gamma_2 = \cos^{-1}\left[\frac{(a_o)^2 + (ac_o)^2 - (ab_o)^2}{(2)(a_o)(ab_o)}\right] = 23.4^\circ$$

$$\gamma_3 = \cos^{-1}\left[\frac{(ab_o)^2 + (ac_o)^2 - (a_o)^2}{(2)(ab_o)(ac_o)}\right] = 140.5^\circ$$

Note: $\gamma_1 + \gamma_2 + \gamma_3 = 180^\circ$

Now, a, b, and c can be recast in terms of h. Specifically,

$$a = h\frac{\cos(\gamma_1)}{\tan(\alpha_3)} + h\frac{\cos(\gamma_2)}{\tan(\alpha_1)} = \left[\frac{\cos(\gamma_1)}{\tan(\alpha_3)} + \frac{\cos(\gamma_2)}{\tan(\alpha_1)}\right]h = l_a h \quad ; \; l_a = 0.57$$

$$b = h\frac{\cos(\theta_1)}{\tan(\alpha_2)} + h\frac{\cos(\theta_2)}{\tan(\alpha_3)} = \left[\frac{\cos(\theta_1)}{\tan(\alpha_2)} + \frac{\cos(\theta_2)}{\tan(\alpha_3)}\right]h = l_b h \quad ; \; l_b = 0.72$$

$$c = h\frac{\cos(\beta_1)}{\tan(\alpha_1)} + h\frac{\cos(\beta_2)}{\tan(\alpha_2)} = l_c h \quad ; \; l_c = 0.48$$

Recall that the volume of the rock block can be calculated from the following (see page 28 of this notebook):

$$V = \frac{1}{3} h \Delta$$

where

$$\Delta = [s(s-a)(s-b)(s-c)]^{1/2}$$

$$s = \frac{a+b+c}{2}$$

Writing s as a function of h,

$$s(h) = \left(\frac{l_a + l_b + l_c}{2}\right) h$$

then

$$(s-a) = \left(\frac{l_a + l_b + l_c}{2}\right) h - l_a h$$

$$= \left(\frac{l_b + l_c - l_a}{2}\right) h$$

$$(s-b) = \left(\frac{l_a + l_c - l_b}{2}\right) h$$

$$(s-c) = \left(\frac{l_a + l_b - l_c}{2}\right) h$$

$$\therefore \quad \Delta = \left[\left(\frac{l_a+l_b+l_c}{2}\right)\left(\frac{l_b+l_c-l_a}{2}\right)\left(\frac{l_a+l_c-l_b}{2}\right)\left(\frac{l_a+l_b-l_c}{2}\right)\right]^{1/2} h^2$$

$$= [(l_a+l_b+l_c)(l_b+l_c-l_a)(l_a+l_c-l_b)(l_a+l_b-l_c)]^{1/2} \frac{h^2}{4}$$

$$\therefore \quad V = \frac{1}{12} [(l_a+l_b+l_c)(l_b+l_c-l_a)(l_a+l_c-l_b)(l_a+l_b-l_c)]^{1/2} h^3$$

$$\therefore \quad h = \left\{\frac{12V}{[(l_a+l_b+l_c)(l_b+l_c-l_a)(l_a+l_c-l_b)(l_a+l_b-l_c)]^{1/2}}\right\}^{1/3}$$

$$\therefore \quad h = 2.8\, V^{1/3}$$

$$= 2.8 \left(\frac{m}{\rho}\right)^{1/3}$$

The rock density, from page 26 of this notebook, is 2,700 kg/m³ (2.7 tonnes/m³).

Valid Rock Block Dimensions for a Given Mass

Mass (tonnes)	Volume (m³)	h (m)	a (m)	b (m)	c (m)	
5	1.85	3.44	1.96	2.47	1.65	
10	3.70	4.33	2.47	3.12	2.08	
15	5.56	4.96	2.83	3.57	2.38	
20	7.41	5.46	3.11	3.83	2.62	
25	9.26	5.88	3.35	4.23	2.82	
30	11.11	6.25	3.56	4.50	3.00	
35	12.96	6.58	3.75	4.74	3.16	
40	14.81	6.88	3.92	4.95	3.30	
45	16.67	7.15	4.08	5.15	3.43	
50	18.52	7.41	4.22	5.33	3.56	
55	20.37	7.65	4.36	5.51	3.67	
60	22.22	7.87	4.49	5.67	3.78	
65	24.07	8.08	4.61	5.82	3.88	
70	25.93	8.29	4.72	5.97	3.98	
75	27.78	8.48	4.83	6.11	4.07	
80	29.63	8.66	4.94	6.24	4.16	
1	0.37	2.01	1.15	1.45	0.97	Added 4/21/2000
2	0.74	2.53	1.44	1.82	1.22	

Doug [illegible] 4/6/2000

Constitutive Model for the Rock Block

From the RDTME IRSR the elastic mechanical properties for the emplacement drift rock mass are:

Modulus of Elasticity, $E = 32.6$ GPa
Poisson's Ratio, $\nu = 0.21$

Note that these properties are ~~derived~~ DJ 6/21/2000 applicable/appropriate/ correspond to rock mass behavior, not intact rock. These properties are being used for the analysis because they are considered to be more representative of how the rock block will behave during impact with the drip shield or waste package.

The yield surface for the rock mass is assumed to be represented by the Mohr-Coulomb model. Because ABAQUS/Explicit does not provide the option of using the Mohr-Coulomb model directly, it must be modeled using the Drucker-Prager theory. This requires the various constants of the Drucker-Prager model to be adjusted such that the Mohr-Coulomb yield surface is ultimately represented. Referring to DJ 9/6/2000 the ABAQUS/Explicit User's Manual, Volume 1, Version 5.8; the linear Drucker-Prager yield surface can be written as

$$F = t - p\tan(\beta) - d = 0 \quad ; \text{ Drucker-Prager Yield Surface}$$

where

$$t = \frac{1}{2} q \left[1 + \frac{1}{K} - \left(1 - \frac{1}{K}\right)\left(\frac{r}{q}\right)^3 \right]$$

$$p = \frac{-1}{3}\,\mathrm{trace}(\sigma) \quad ; \text{ equivalent pressure stress}$$

$$q = \left[\frac{3}{2}(S:S)\right]^{1/2} \quad ; \text{ Mises equivalent stress}$$

$$r = \left(\frac{9}{2} S\cdot S:S\right)^{1/3} \quad ; \text{ third invariant of deviatoric stress}$$

$S = \sigma + pI$; deviatoric stress
$\sigma \equiv$ Cauchy stress
$I \equiv$ identity matrix
$\beta \equiv$ the slope of the linear yield surface in the p-t stress plane and is commonly referred to as the friction angle of the material
$d \equiv$ cohesion of the material
$K \equiv$ the ~~yield~~ DJ 9/6/2000 ratio of the yield stress in triaxial tension to the yield stress in triaxial compression and, thus, controls the dependence of the yield surface on the value of the intermediate principal stress.

Moreover,

$$d = \left[1 - \frac{1}{3}\tan(\beta)\right]\sigma_c \quad ; \text{ if hardening is defined by the uniaxial compression yield stress, } \sigma_c.$$

$$= \left[\frac{1}{K} + \frac{1}{3}\tan(\beta)\right]\sigma_t \quad ; \text{ if hardening is defined by the uniaxial tension yield stress, } \sigma_t.$$

$$= \frac{\sqrt{3}}{2}\tau\left(1 + \frac{1}{K}\right) \quad ; \text{ if hardening is defined by the cohesion}$$

Unlike Drucker-Prager, the Mohr-Coulomb yield surface is not dependent on the intermediate principal stress, i.e. σ_2. Specifically, from the ABAQUS/Explicit User's Manual,

$$F = s + \sigma_m \sin(\phi) - c\cos(\phi) = 0 \quad ; \text{ Mohr-Coulomb Yield Surface}$$

where

$$s = \frac{1}{2}(\sigma_1 - \sigma_3)$$

$$\sigma_m = \frac{1}{2}(\sigma_1 + \sigma_3)$$

$c = 2.54(10^6)$ Pa ; Mohr-Coulomb cohesion
$\phi = 34.4°$; Mohr-Coulomb friction angle

Note that c and ϕ are derived from the rock mass quality measurements for the emplacement drift rock (See the RDTME IRSR). Furthermore, it needs to be pointed out that these values are diffent from the values used by DOE.

Substituting s and σ_m into the Mohr-Coulomb yield surface criterion and solving for σ_3 gives

$$\sigma_3 = \frac{\{\sigma_1[1+\sin(\phi)] - 2c\cos(\phi)\}}{[1-\sin(\phi)]}$$

To define the Drucker-Prager yield surface, the β and K parameters must be quantified. Setting $K=0.78$ will provide the desired shape of the yield surface (see the ABAQUS/Explicit User's Manual). β is determined as follows.

Because the rock mass Mohr-Coulomb properties, c and ϕ, were determined from rock mass quality tests analogous to compression test conditions, i.e. $0>(\sigma_1=\sigma_2)>\sigma_3$, then the hardening and Drucker-Prager cohesion will be determined using the uniaxial compression yield stress. In particular,

$$d = \left[1 - \frac{1}{3}\tan(\beta)\right]\sigma_c$$

From "Fundamentals of Rock Mechanics, 3'rd ed.," J.C. Jaeger and N.G.W. Cook, p. 97, Chapman and Hall, London; the uniaxial compression yield stress can be approximated/calculated using the following relationship,

$$\sigma_1 = -2c\tan(\alpha) + \sigma_3\tan^2(\alpha) \quad ; \text{ assuming } \sigma_1 \text{ and } \sigma_3 \text{ are negative values}$$

and $\sigma_1 = \sigma_c$ when $\sigma_3 = 0$.

$$\therefore \sigma_c = \sigma_1\Big|_{\sigma_3=0} = -2c\tan(\alpha)$$

where

$$\alpha = \frac{\pi}{4} + \frac{\phi}{2}$$

Using $c = 2.54(10^6)\ N/m^2$ and $\phi = 34.4°$,

$$\sigma_c = -9.635(10^6)\ N/m^2$$

Now, substituting the relationships for d and σ_c into the Drucker-Prager yield surface criterion gives

$$t - p\tan(\beta) - d = 0$$

$$t - p\tan(\beta) + \left[1 - \frac{1}{3}\tan(\beta)\right]2c\tan(\alpha) = 0$$

Solving for $\tan(\beta)$ we have

$$\tan(\beta) = \frac{[6c\tan(\alpha) + 3t]}{[3p + 2c\tan(\alpha)]}$$

Recognizing that t and p are functions of the principal stresses, σ_1, σ_2, and σ_3, some assumptions must be made as to their potential values. First, recall that the Mohr-Coulomb yield surface allowed writing σ_3 in terms of σ_1 (see p. 36 of this scientific notebook). In addition, because the rock mass quality tests were performed under compression test conditions where $0>(\sigma_1=\sigma_2)>\sigma_3$, it will be assumed that $\sigma_1 = \sigma_2$. As a result, $\tan(\beta)$ is strictly a function of σ_1.

To determine the sensitivity of β to variations in σ_1, a spreadsheet was used to calculate β for a broad range of σ_1. The results are shown on p. 38 of this scientific notebook. Note that, in terms of the principal stresses

$$p = \frac{-1}{3}(\sigma_1 + \sigma_2 + \sigma_3)$$

$$q = (\sigma_1^2 + \sigma_2^2 + \sigma_3^2 - \sigma_1\sigma_2 - \sigma_3\sigma_1 - \sigma_2\sigma_3)^{1/2}$$

$$r = \left[\frac{1}{2}(2\sigma_1^3 + 2\sigma_2^3 + 2\sigma_3^3 - 3\sigma_1\sigma_2^2 - 3\sigma_1\sigma_3^2 - 3\sigma_1^2\sigma_2 - 3\sigma_2\sigma_3^2 - 3\sigma_1^2\sigma_3 - 3\sigma_2^2\sigma_3 + 12\sigma_1\sigma_2\sigma_3)\right]^{1/3}$$

Cohesion = 2.54 MPa
ϕ = 34.4°

sig1 (Pa)	sig2 (Pa)	sig3 (Pa)	p	q	r	t	Beta (deg.)
0.00	0.00	-9635077.35 = σ_c	3211692.45	9635077.35	-9635077.35	9635077.35	71.57
-100000.00	-100000.00	-9994812.59	3398270.86	9894812.59	-9894812.59	9894812.59	71.43
-200000.00	-200000.00	-10354547.84	3584849.28	10154547.84	-10154547.84	10154547.84	71.29
-300000.00	-300000.00	-10714283.08	3771427.69	10414283.08	-10414283.08	10414283.08	71.15
-400000.00	-400000.00	-11074018.32	3958006.11	10674018.32	-10674018.32	10674018.32	71.02
-500000.00	-500000.00	-11433753.56	4144584.52	10933753.56	-10933753.56	10933753.56	70.89
-600000.00	-600000.00	-11793488.81	4331162.94	11193488.81	-11193488.81	11193488.81	70.76
-700000.00	-700000.00	-12153224.05	4517741.35	11453224.05	-11453224.05	11453224.05	70.64
-800000.00	-800000.00	-12512959.29	4704319.76	11712959.29	-11712959.29	11712959.29	70.51
-900000.00	-900000.00	-12872694.53	4890898.18	11972694.53	-11972694.53	11972694.53	70.39
-1000000.00	-1000000.00	-13232429.78	5077476.59	12232429.78	-12232429.78	12232429.78	70.27
-1100000.00	-1100000.00	-13592165.02	5264055.01	12492165.02	-12492165.02	12492165.02	70.15
-1200000.00	-1200000.00	-13951900.26	5450633.42	12751900.26	-12751900.26	12751900.26	70.03
-1300000.00	-1300000.00	-14311635.50	5637211.83	13011635.50	-13011635.50	13011635.50	69.91
-1400000.00	-1400000.00	-14671370.75	5823790.25	13271370.75	-13271370.75	13271370.75	69.80
-1500000.00	-1500000.00	-15031105.99	6010368.66	13531105.99	-13531105.99	13531105.99	69.68
-1600000.00	-1600000.00	-15390841.23	6196947.08	13790841.23	-13790841.23	13790841.23	69.57
-1700000.00	-1700000.00	-15750576.47	6383525.49	14050576.47	-14050576.47	14050576.47	69.46
-1800000.00	-1800000.00	-16110311.72	6570103.91	14310311.72	-14310311.72	14310311.72	69.36
-1900000.00	-1900000.00	-16470046.96	6756682.32	14570046.96	-14570046.96	14570046.96	69.25
-2000000.00	-2000000.00	-16829782.20	6943260.73	14829782.20	-14829782.20	14829782.20	69.14
-2100000.00	-2100000.00	-17189517.44	7129839.15	15089517.44	-15089517.44	15089517.44	69.04
-2200000.00	-2200000.00	-17549252.68	7316417.56	15349252.68	-15349252.68	15349252.68	68.94
-2300000.00	-2300000.00	-17908987.93	7502995.98	15608987.93	-15608987.93	15608987.93	68.84
-2400000.00	-2400000.00	-18268723.17	7689574.39	15868723.17	-15868723.17	15868723.17	68.74
-2500000.00	-2500000.00	-18628458.41	7876152.80	16128458.41	-16128458.41	16128458.41	68.64
-2600000.00	-2600000.00	-18988193.65	8062731.22	16388193.65	-16388193.65	16388193.65	68.54
-2700000.00	-2700000.00	-19347928.90	8249309.63	16647928.90	-16647928.90	16647928.90	68.45
-2800000.00	-2800000.00	-19707664.14	8435888.05	16907664.14	-16907664.14	16907664.14	68.35
-2900000.00	-2900000.00	-20067399.38	8622466.46	17167399.38	-17167399.38	17167399.38	68.26
-3000000.00	-3000000.00	-20427134.62	8809044.87	17427134.62	-17427134.62	17427134.62	68.17
-3100000.00	-3100000.00	-20786869.87	8995623.29	17686869.87	-17686869.87	17686869.87	68.08
-3200000.00	-3200000.00	-21146605.11	9182201.70	17946605.11	-17946605.11	17946605.11	67.99
-3300000.00	-3300000.00	-21506340.35	9368780.12	18206340.35	-18206340.35	18206340.35	67.90
-3400000.00	-3400000.00	-21866075.59	9555358.53	18466075.59	-18466075.59	18466075.59	67.81
-3500000.00	-3500000.00	-22225810.84	9741936.95	18725810.84	-18725810.84	18725810.84	67.72
-3600000.00	-3600000.00	-22585546.08	9928515.36	18985546.08	-18985546.08	18985546.08	67.64
-3700000.00	-3700000.00	-22945281.32	10115093.77	19245281.32	-19245281.32	19245281.32	67.55
-3800000.00	-3800000.00	-23305016.56	10301672.19	19505016.56	-19505016.56	19505016.56	67.47
-3900000.00	-3900000.00	-23664751.80	10488250.60	19764751.80	-19764751.80	19764751.80	67.39
-4000000.00	-4000000.00	-24024487.05	10674829.02	20024487.05	-20024487.05	20024487.05	67.31
-4100000.00	-4100000.00	-24384222.29	10861407.43	20284222.29	-20284222.29	20284222.29	67.23
-4200000.00	-4200000.00	-24743957.53	11047985.84	20543957.53	-20543957.53	20543957.53	67.15
-4300000.00	-4300000.00	-25103692.77	11234564.26	20803692.77	-20803692.77	20803692.77	67.07
-4400000.00	-4400000.00	-25463428.02	11421142.67	21063428.02	-21063428.02	21063428.02	66.99
-4500000.00	-4500000.00	-25823163.26	11607721.09	21323163.26	-21323163.26	21323163.26	66.92
-4600000.00	-4600000.00	-26182898.50	11794299.50	21582898.50	-21582898.50	21582898.50	66.84
-4700000.00	-4700000.00	-26542633.74	11980877.91	21842633.74	-21842633.74	21842633.74	66.77
-4800000.00	-4800000.00	-26902368.99	12167456.33	22102368.99	-22102368.99	22102368.99	66.69
-4900000.00	-4900000.00	-27262104.23	12354034.74	22362104.23	-22362104.23	22362104.23	66.62
-5000000.00	-5000000.00	-27621839.47	12540613.16	22621839.47	-22621839.47	22621839.47	66.55
-5100000.00	-5100000.00	-27981574.71	12727191.57	22881574.71	-22881574.71	22881574.71	66.48

As can be seen from the spreadsheet, β will vary with the choice of σ_1. But, because the falling rock block will experiance stress states upon impact that will have relatively small confining pressures, a value of 70° was assumed for β.

The final parameter to be calculated for the rock constitutive model is the Drucker-Prager dilation angle in the p-t plane for establishing the "plastic" flow potential (see the ABAQUS/Explicit User's Manual). For the purpose of this analysis it was assumed that

$$\psi = \frac{\beta}{2} \quad ; \text{ Drucker-Prager Dilation Angle.}$$

In terms of the uniaxial compression stress, the stress-strain curve for the rock block mass is (note that perfectly plastic behavior is assumed after yielding).

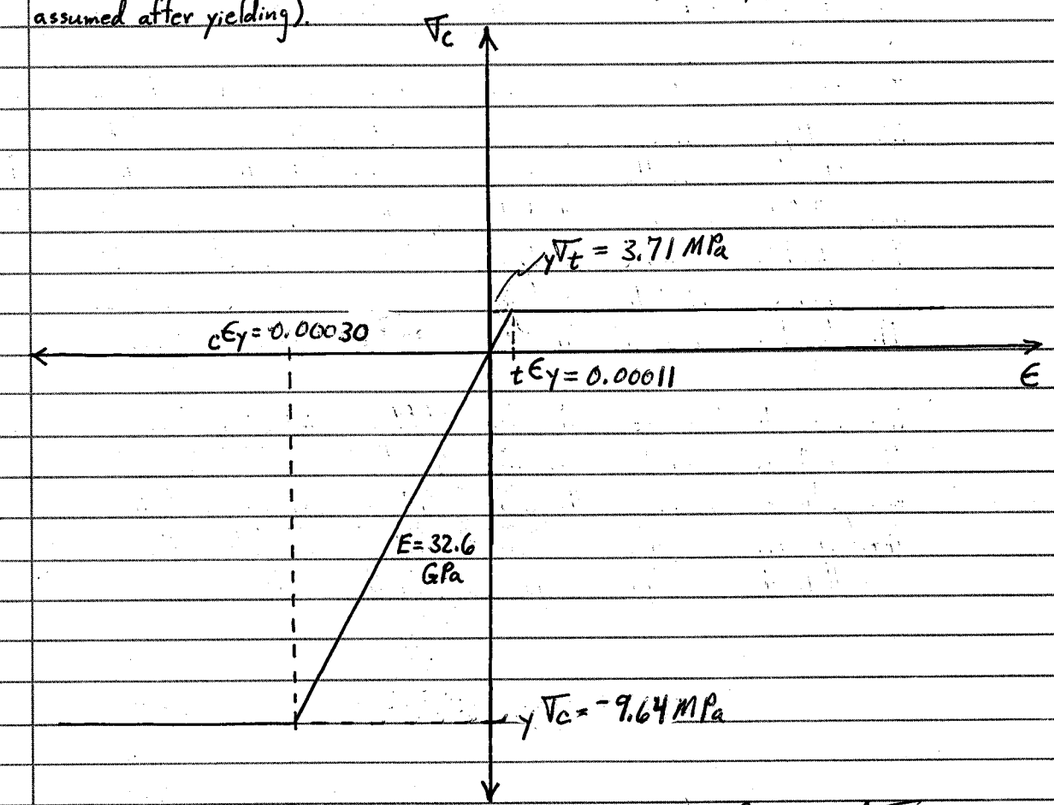

Doug Stute 4/12/2000

Initial Finite Element Analysis Objectives and Methodology

Having identified and developed the available material properties and concomitant constitutive relationships, respectively, for the drip shield, waste package, and rock blocks; it has been determined that ABAQUS/Explicit, Ver. 5.8, is capable of simulating seismically induced rockfall on the engineered barrier system components of the proposed geologic repository. ABAQUS/Explicit, Ver. 5.8, is a general purpose finite element analysis program developed by Hibbitt, Karlson, and Sorenson, Inc. (HKS). It employs an explicit numerical time integration methodology that is ideally suited for performing the solution of finite element based numerical approximations of short duration dynamic events.

The objective of the rockfall analysis is to develop a methodology that can be used to assess the capabilities of the individual engineered barrier components to withstand rockfall without loss of function. As a first attempt, rock block impacts with the drip shield will be addressed.

The finite element analysis models will be pre- and post-processed using HyperMesh on a personal computer with a Windows NT operating system. The local area network name for this computer is Galit. HyperMesh is a component of the HyperWorks program developed by Altair Engineering. The actual finite element analyses will be performed on a Sun Enterprise workstation configured with four microprocessors. The local area network name for this workstation is Vulcan.

When constructing the finite element (FE) model of the drip shield (DS) the first and foremost requirement is that the individual FE type used is capable of capturing all the significant physical aspects of the problem, given the boundary and load conditions to be simulated. Based on the overall thickness to length aspect ratio of the structure (i.e., 0.02/5.50) the first inclination would be to use shell elements to discretize the structure. Shell elements within ABAQUS, however, are not formulated to capture in-plane bending or out of plane normal stresses relative to the shell surface. Because certain parts of the structure may experience in-plane bending moments, and out of plane normal stresses are anticipated to be significant in the

area of the contact interface between the rock block and DS, it was determined that shell elements are inappropriate for the task at hand.

According to the ABAQUS/Explicit User's Manual, solid continuum elements can be used for complex nonlinear analyses involving contact, plasticity, and large deformations. As with shell elements, solid elements are reduced integration elements. Care must be taken to ensure that hourglassing does not occur when using reduced-integration elements. Hourglassing can be avoided by using an adequate mesh density within the model or by introducing artificial numerical damping to suppress the hourglass modes. Because the inappropriate use of artificial damping may result in an excessively stiff response by the structure, it was decided that the problem of hourglassing would be addressed by using an adequately defined mesh.

Even though the vast majority of the DS will experience only membrane stresses after impact by the rock block, bending and out of plane normal stresses will be the dominating factor in the immediate area of the DS and rock block impact zone. Because pure-bending cannot be supported by a single hexahedral element, at least two elements should be used through the thickness of the DS. Ideally, each solid element would have a 1"x 1x 1 dimensional aspect ratio. Given the overall dimensions of the DS and assuming two elements through the 2cm thickness, nearly 542,000 hexahedral elements would be required in the construction of the FE model. Because of limited computational resources, this aspect ratio will initially be assumed to be 1x 4x 4 cm for each individual element.

DH 6/21/2000

Symmetry was not considered ~~as a~~ to be a viable alternative for reducing the size of the DS FE model because the rock block shape is not symmetric and its point of impact with the DS may not be at a point where symmetry boundary conditions may be applied.

A Classical metal plasticity constitutive relationship will be assumed to represent the behavior of Grade 7 Titanium. Because the yield surface for Ti-7 is expected to behave in an isotropic manner, a Von Mises yield surface will be used. The effects of strain rate will not be considered at this time.

To establish a first approximation of the energy dissipated by the rock block during impact with the DS, the material will be modeled as ~~a~~ DJ 9/6/2000 perfectly plastic beyond the yield stress. Note that the Drucker-Prager constitutive relationship was constructed to account for the different rock strengths in tension and compression (see p. 34 of this scientific notebook).

The size and shape of the rock block to be used in the analysis was derived from Key block theory (see p. 26 of this report). Using the tetrahedral rock block shape derived from this theory will enable our assessment of the level of conservatism achieved by assuming a spherical rock block shape. To date, DOE has consistently used spherical rock block shapes to perform their rockfall analyses.

Unlike the DS, where shell elements was an option, the relative dimensions of the rock block necessitates the use of solid elements. What must be considered is the kinematic requirements of the rock block interacting with the surface of the DS and the high strain gradients generated at the time of impact. To address these issues, the dimensions of an individual element at the base of the rock block will be 2 × 2 × 2 cm. The total number of elements, if uniformly sized throughout the rock block, would be extremely high. To minimize the total number of elements required to mesh the rock block, the rock block will be meshed in layers, where the thickness of each layer is increased as an exponential function of its distance from the base of the rock block. Elements created on any given layer will have a 1 × 1 × 1 dimensional aspect ratio. To avoid numerical stress wave echos caused by sudden changes in mesh density, care will be taken to ensure that no layer thickness will be greater than 1.1 times any neighboring layer. The surfaces defining the interface between each of these layers will be "tied" together using a special ABAQUS contact pair definition.

Doug Ruth 4/18/2000

Two sets of three relatively soft springs, one spring within each set for one of the three dimensions of the model, will be used to "constrain" the free falling rock block so that an ill-conditioned stiffness matrix can be avoided. This approach will restrict all possible rigid body translations and rotations without influencing the results of the simulation so long as the springs are sufficiently soft. The magnitude of the spring constant for each of the six springs will be 50 N/m (0.29 lb/in).

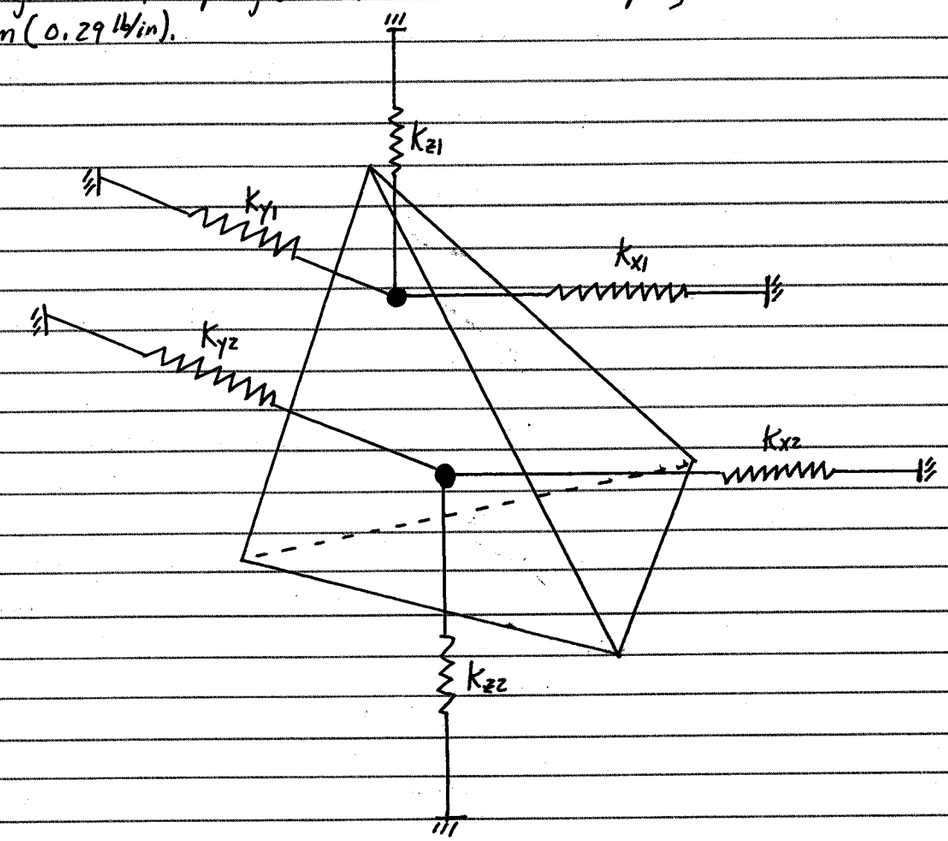

Doug Ruth 4/19/2000

It is not clear at this time if combining ground motion effects with seismically induced rockfall will have a significant influence on the response of the DS. As a first attempt to assess these effects, each DS and rock block scenario will be analyzed with and without a simplified accounting of the ground motion. Because it is assumed that the rock block impacting the DS was dislodged from the emplacement drift roof by way of seismic ground motion, it must also be reasonably assumed that the rock block will have some initial vertical velocity when it begins to fall. Allowing for an initial velocity and variable fall height: DJ 6/21/2000

$$g = \frac{d^2s}{dt^2}$$; $g \equiv$ acceleration due to gravity; $s \equiv$ distance travelled by the falling rock block; $t \equiv$ elapsed time

$$\frac{ds}{dt} = v = gt + C_0$$; $v \equiv$ velocity of the falling rock block; $C_0 \equiv$ arbitrary constant of integration

$$s = h = \frac{1}{2}gt^2 + C_0 t + C_1$$; $h \equiv$ total distance travelled by the rock block before impacting the DS; $C_1 \equiv$ arbitrary constant of integration.

$$s\big|_{t=0} = 0 \longrightarrow C_1 = 0$$

$$v\big|_{t=0} = V_0 \longrightarrow C_0 = V_0$$

$$\therefore \quad v = gt + V_0$$

$$\therefore \quad s = \frac{1}{2}gt^2 + V_0 t$$

The time required to fall a distance h is

$$h = \frac{1}{2}gt^2 + V_0 t$$

$$\frac{1}{2}gt^2 + V_0 t - h = 0$$

Using the quadratic formula,

$$t = \frac{-V_0 \pm \left[V_0^2 - 4(\tfrac{1}{2}g)(-h)\right]^{1/2}}{2(\tfrac{1}{2}g)}$$

$$= \frac{-V_0 \pm \left[V_0^2 + 2gh\right]^{1/2}}{g}$$

Substituting this result into the velocity equation gives

$$V = \pm\left[V_0^2 + 2gh\right]^{1/2}$$; velocity of the rock block when it impacts the drip shield after falling a distance h and having an initial velocity of V_0.

Table 7-1 of the Probabilistic Seismic Hazard Analyses for Fault Displacement and Vibratory Ground Motion at Yucca Mountain, Nevada, indicates that a peak vertical ground velocity of 0.234 m/s has an annual probability of exceedance equal to 10^{-4}. The corresponding peak horizontal ground velocity is 0.472 m/s. These peak values refer to the maximum velocities for frequencies 100 Hz and above. These peak ground velocities do not necessarily correspond to the maximum ground velocities. Because the technical basis for use of these, or any other, values as appropriate design criteria has yet to be established, it has been assumed for the present that the maximum vertical ground velocity is 1 m/s. Note that the horizontal component will not be considered in the simulation. Letting

$$h = 1.25\,\text{m}$$
$$V_0 = 1\,\text{m/s}$$
$$g = 9.81\,\text{m/s}^2$$

DJ 6/21/2000

the impact ~~vector~~ velocity is

$$V = \left[(1\,\text{m/s})^2 + (2)(9.81\,\text{m/s}^2)(1.25\,\text{m})\right]^{1/2}$$
$$= 5.05\,\text{m/s}$$

If the initial downward velocity is not considered, the impact velocity is reduced to 4.95 m/s.

Although the velocity of the rock block at the time of impact is not affected significantly by the ground motion, the interaction between the DS and rock block may be influenced by the seismic excitation at the base of the DS. For structures with natural frequencies below 33 Hz, resonance can play a major role in the way the structure will respond to seismic excitation. In the absence of a time-history or response spectrum representation of the expected seismic activity for the repository horizon, potential dynamic amplification effects cannot be studied. As a result, the ground motion will simply be modeled by setting the vertical velocity of the entire DS to the assumed vertical ground motion velocity. Transient acceleration effects are removed from the system and the DS will be in a steady-state condition at the time of impact with the rock block. Just as the rock block impacts the DS, the velocities of the individual nodes of the DS are freed from all displacement, velocity, and acceleration constraints with the exceptions of the nodes at the base of the DS. The nodes at the base of the DS are required to follow the time history of the ground motion. Because the duration of the DS and rock block impact event is not known, the vertical ground motion velocity will be considered to be constant throughout the analysis. In addition, the nodes at the base of the DS will be constrained from any horizontal translations and all rotations. In other words, the base of the DS is completely fixed to the invert.
If the DS is to be a free-standing structure on the invert, the boundary conditions at the base of the DS will have to be changed correspondingly. A free-standing DS will have a very different response from one that is fixed to the invert.

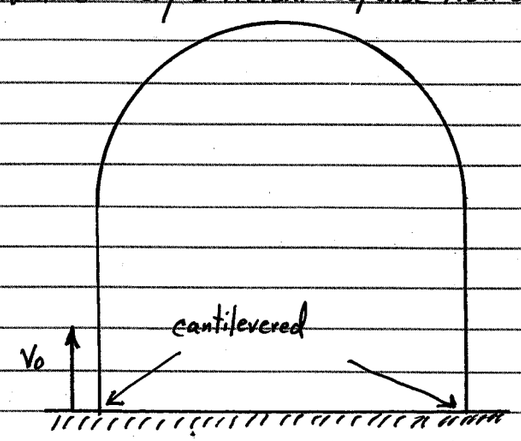

Doug Ate 4/20/2000

At the request of Asad Chowdhury, the rock block sizes to be used for the analysis will be reduced to 1 and 2 tonnes.

Doug Ate 4/21/2000

To limit the vertical deflection that the DS can experiance, the WP will be included in the analysis as an analytical cylindrical surface that is perfectly rigid. This allows the presence of the WP without having to explicitly model it with typical finite elements. The WP will move upward at the same constant velocity as the DS.

Because the immediate objective is to develop a methodology capable of simulating the DS and rock block impact event and attempt to identify, in a qualitative manner, certain aspects of the rockfall problem that may play a role in assessing how this type of mechanical disruption can affect the DS's ability to perform its intended function; the effects of rockblock size, rock block mesh density, and vertical ground motion velocity will be investigated. The following analysis permutations will be performed.

1-tonne Rock Block				2-tonne Rock Block			
Fine Mesh Rock		Coarse Mesh		Fine Mesh		Coarse Mesh	
Ground Motion	Ground Motion	Ground Motion	Ground Motion	Ground Motion	Ground Motion	Ground Motion	Ground Motion
0 m/s	1 m/s	0 m/s	1 m/s	0 m/s	1 m/s	0 m/s	1 m/s

Doug Ate 4/21/2000

Preliminary Finite Element Analysis Results

None of the fine mesh models ran to completion because of numerical problems. These numerical problems were the result of individual rock block elements that are part of the DS - rock block contact interface experiencing high deformation rate to wave speed ratios. The high deformation rate to wave speed ratio has been shown to be a good indicator for predicting imminent unrealistic element deformation or collapse. This may be interpreted as a manifestation of the rock block beginning to fracture and splinter. As can be seen from ~~to~~ DJ 6/21/2000 the figure on p. 49 of this notebook, the deformation at the rock block vertex is becoming quite severe and the velocity, which is horizontally oriented, has become quite high. The ability to capture this effect is desirable in that crushing and fracturing of the rock can be predicted, it adds additional complexity to the simulation because an appropriate failure criteria must be developed so these elements can be removed from the model before the simulation is terminated prematurely.

The tables on pages 50 and 51 of this scientific notebook are compilations of the Kinetic Energy, Total Energy, Absolute DS displacement, and Relative Clearance between the DS + WP as functions of time. Just before impact, the Total Energy of the system is represented by the Kinetic ~~of th~~ Energy DJ 6/21/2000 of the rock block and drip shield. The following table summarizes the actual volume and mass of the 1- and 2-tonne rock blocks and DS.

	Volume (m^3)	Mass (kg)
1-tonne Rock Block	0.390	1053.0000
2-tonne Rock Block	0.736	1987.2000
Drip Shield	0.542	2445.5040

The next table compiles the contribution to the Total Energy of each individual components Kinetic Energy in terms of the ground motion.

	Kinetic Energy	
	0 m/s	1 m/s
1-tonne Rock Block	12.9 kJ	13.4 kJ
2-tonne Rock Block	24.3 kJ	25.3 kJ
Drip Shield	0	1.22 kJ

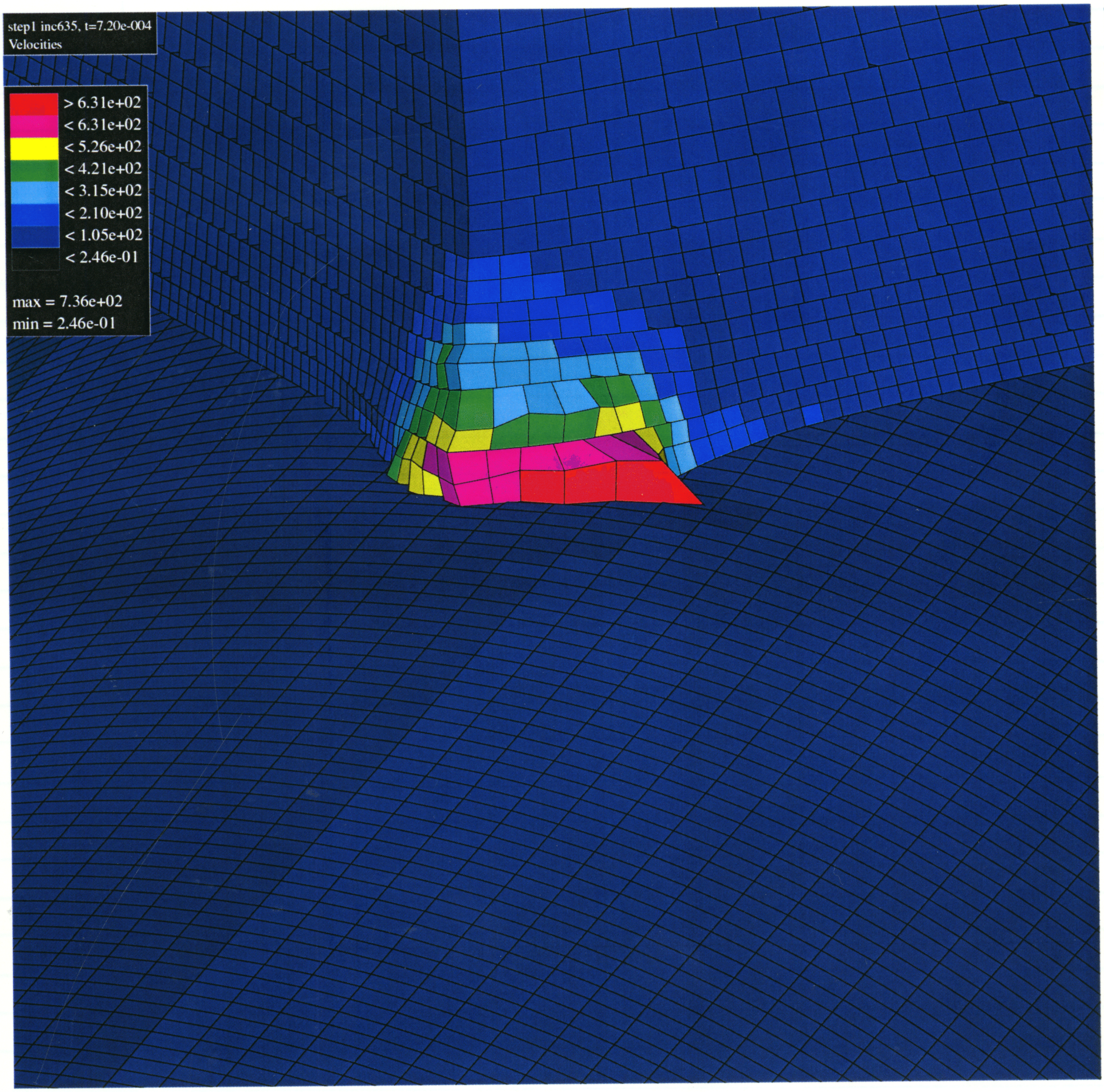

Velocity (m/s) contour plot. 1-tonne rock block with fine mesh and 1 m/s ~~vel~~ vertical velocity ground motion.

DA 6/21/2000

1 tonne Rock

Time (ms)	Fine Mesh, Base Motion = 0 m/s: Kinetic Energy (x 10^4 Joules)	Total Energy (x 10^4 Joules)	Absolute Displacement (mm)	DS-WP Clearance (mm)	Fine Mesh, Base Motion = 1 m/s: Kinetic Energy (x 10^4 Joules)	Total Energy (x 10^4 Joules)	Absolute Displacement (mm)	DS-WP Clearance (mm)	Coarse Mesh, Base Motion = 0 m/s: Kinetic Energy (x 10^4 Joules)	Total Energy (x 10^4 Joules)	Absolute Displacement (mm)	DS-WP Clearance (mm)	Coarse Mesh, Base Motion = 1 m/s: Kinetic Energy (x 10^4 Joules)	Total Energy (x 10^4 Joules)	Absolute Displacement (mm)	DS-WP Clearance (mm)
0.00	1.2910	1.2910	0.0000	55.5000	1.4660	1.4660	0.0000	55.5000	1.2910	1.2910	0.0000	55.5000	1.2910	1.2910	0.0000	55.5000
1.00	1.2050	1.2910	-4.8940	50.6060	1.3530	1.4660	-4.4660	50.0340	1.2080	1.2910	-4.8610	50.8390	1.3530	1.4660	-4.4660	50.0340
2.00	1.1330	1.2910	-9.0290	46.4710	1.2510	1.4660	-9.1980	44.3020	1.1270	1.2910	-9.2530	46.2470	1.2510	1.4660	-9.1980	44.3020
3.00	1.0370	1.2910	-13.4800	42.0200	1.0930	1.4660	-13.3400	39.1600	1.0440	1.2910	-13.1200	42.3800	1.0930	1.4660	-13.3400	39.1600
4.00	0.9436	1.2910	-17.3900	38.1100	0.9549	1.4660	-17.1500	34.3500	0.9451	1.2910	-17.2800	38.2400	0.9549	1.4660	-17.1500	34.3500
5.00	0.8676	1.2910	-20.9700	34.5300	0.8491	1.4660	-20.6100	29.8900	0.8673	1.2910	-20.9100	34.5900	0.8491	1.4660	-20.6100	29.8900
6.00	0.8247	1.2910	-24.3100	31.1900	0.7982	1.4660	-23.6200	25.8800	0.8240	1.2910	-24.2400	31.2500	0.7982	1.4660	-23.6200	25.8800
7.00	0.7967	1.2910	-27.2700	28.2300	0.7642	1.4660	-26.5200	21.9800	0.7971	1.2910	-27.2200	28.2800	0.7642	1.4660	-26.5200	21.9800
8.00	0.7700	1.2910	-29.8000	25.7000	0.7471	1.4660	-28.5200	18.9800	0.7706	1.2910	-29.8800	25.6200	0.7471	1.4660	-28.5200	18.9800
9.00	0.7395	1.2910	-32.1000	23.4000	0.7284	1.4660	-30.6000	15.9000	0.7439	1.2910	-31.9600	23.5400	0.7284	1.4660	-30.6000	15.9000
10.00	0.7026	1.2910	-34.1900	21.3100	0.6970	1.4660	-32.1000	13.4000	0.7068	1.2910	-34.0300	21.4700	0.6970	1.4660	-32.1000	13.4000
11.00	0.6608	1.2910	-36.0300	19.4700	0.6674	1.4660	-33.3700	11.1300	0.6646	1.2910	-35.8300	19.6700	0.6674	1.4660	-33.3700	11.1300
12.00	45.0200	2.5910	-37.5400	17.9600	0.6455	1.4660	-34.4400	9.0600	0.6264	1.2910	-37.2900	18.2100	0.6455	1.4660	-34.4400	9.0600
13.00					0.6439	1.4660	-35.2600	7.2400	0.5910	1.2910	-38.8200	16.6800	0.6439	1.4660	-35.2600	7.2400
14.00					0.6567	1.4660	-36.0500	5.4500	0.5888	1.2910	-40.2500	15.2500	0.6567	1.4660	-36.0500	5.4500
15.00					0.6741	1.4660	-36.6500	3.8500	0.5559	1.2910	-41.4700	14.0300	0.6741	1.4660	-36.6500	3.8500
16.00					0.6807	1.4660	-37.1500	2.3500	0.5380	1.2910	-42.7200	12.7800	0.6807	1.4660	-37.1500	2.3500
17.00					0.6718	1.4660	-37.4700	1.2500	0.5100	1.2910	-43.7500	11.7500	0.6718	1.4660	-37.4700	1.2500
18.00					1.4790	1.4660	0.0300	0.0300	0.4593	1.2910	-44.7800	10.7200	1.4790	1.4660	0.0300	0.0300
19.00					516.8000	-0.1616	-36.5400	-0.0400	0.3914	1.2910	-45.6300	9.8700	516.8000	-0.1616	-36.5400	-0.0400
20.00									0.3076	1.2910	-46.3800	9.1200				
21.00									0.2156	1.2910	-47.0300	8.4700				
22.00									0.1427	1.2910	-47.4900	8.0100				
23.00									0.0964	1.2910	-47.8800	7.6200				
24.00									0.0622	1.2910	-48.1200	7.3800				
25.00									0.0687	1.2910	-48.2300	7.2700				
26.00									0.0999	1.2910	-48.2600	7.2400				
27.00									0.1438	1.2910	-48.2200	7.2800				
28.00									0.1855	1.2910	-48.1300	7.3700				
29.00									0.2302	1.2910	-47.9800	7.5200				
30.00									0.2897	1.2910	-47.7800	7.7200				
31.00									0.3044	1.2910	-47.5500	7.9500				
32.00									0.3341	1.2910	-47.2500	8.2500				
33.00									0.3667	1.2910	-46.7800	8.7200				
34.00									0.3981	1.2910	-46.1100	9.3900				
35.00									0.4266	1.2910	-45.2700	10.2300				

2 tonne Rock

Time (ms)	Fine Mesh, Base Motion = 0 m/s: Kinetic Energy (x 10^4 Joules)	Total Energy (x 10^4 Joules)	Absolute Displacement (mm)	DS-WP Clearance (mm)	Fine Mesh, Base Motion = 1 m/s: Kinetic Energy (x 10^4 Joules)	Total Energy (x 10^4 Joules)	Absolute Displacement (mm)	DS-WP Clearance (mm)	Coarse Mesh, Base Motion = 0 m/s: Kinetic Energy (x 10^4 Joules)	Total Energy (x 10^4 Joules)	Absolute Displacement (mm)	DS-WP Clearance (mm)	Coarse Mesh, Base Motion = 1 m/s: Kinetic Energy (x 10^4 Joules)	Total Energy (x 10^4 Joules)	Absolute Displacement (mm)	DS-WP Clearance (mm)
0.00	2.4350	2.4350	0.0000	55.5000	2.6570	2.6570	0.0000	55.5000	2.4350	2.4350	0.0000	55.5000	2.6570	2.6570	0.0000	55.5000
1.00	2.3470	2.4350	-4.6210	50.8790	2.5250	2.6570	-5.0070	49.4930	2.2620	2.4350	-4.6620	50.7720	2.5330	2.6570	-4.8380	49.6620
2.00	2.2600	2.4350	-9.5140	45.9860	2.4280	2.6570	-9.4140	44.0860	2.3530	2.4350	-4.7280		2.4630	2.6570	-9.5390	43.9610
3.00	2.1590	2.4350	-13.8700	41.6300	2.2330	2.6570	-14.2500	38.2500					28.0000	2.4120	-15.5500	36.9500
	2.0510	2.4350	-18.1700	37.3300	2.0780	2.6570	-18.4000	33.1000								
	1.9510	2.4350	-22.5200	32.9800	1.9450	2.6570	-22.5600	27.9400								
	1.8860	2.4350	-26.6600	28.8400	1.8640	2.6570	-26.6100	22.8900								
	1.8380	2.4350	-30.2100	25.2900	1.7950	2.6570	-30.2900	18.2100								
	1.7830	2.4350	-34.0200	21.4800	1.7380	2.6570	-33.7200	13.7800								
	1.7290	2.4350	-37.2600	18.2400	1.6860	2.6570	-36.8700	9.6300								
	1.6670	2.4350	-40.3600	15.1400	1.6150	2.6570	-39.7400	5.7600								
	1.6000	2.4350	-43.2500	12.2500	1.5470	2.6570	-42.4600	2.0400								
	1.5320	2.4350	-46.0200	9.4800	1.3020	2.6580	-43.5000	0.0000								
	1.4630	2.4350	-49.0000	6.5000												
	1.4130	2.4350	-51.6100	3.8900												
	1.3710	2.4350	-54.0500	1.4500												
	38.0200	2.5180	-55.5000	0.0000												

Time (ms)
0.00
1.00
2.00
3.00
4.00
5.00
6.00
7.00
8.00
9.00
10.00
11.00
12.00
13.00
14.00
15.00
16.00
17.00
18.00
19.00
20.00
21.00
22.00
23.00
24.00
25.00
26.00
27.00
28.00
29.00
30.00
31.00
32.00
33.00
34.00
35.00

Tallying up the kinetic energy for the different permutations we find that the total system energy has been accounted for in the FE models correctly. Note that the total energy of the system should remain constant throughout the entire simulation. The kinetic energy, on the other hand, will be converted to other forms (e.g. elastic and plastic strain energy). On review of the tables on pages 50 and 51 of this notebook, the total energy of the system begins to change ~~just prior to~~ when DA 6/21/2000 the solution ~~becoming~~ becomes DA 6/21/2000 numerically unstable and terminates prematurely.

Also included in the tables on pages 50 and 51 is the relative displacement/clearance between the DS and WP. A plot of the clearance between the DS + WP as a function of time is provided below. Note that only DA 6/21/2000 the coarse mesh rock block models results are plotted. ~~only~~ DA 6/21/2000

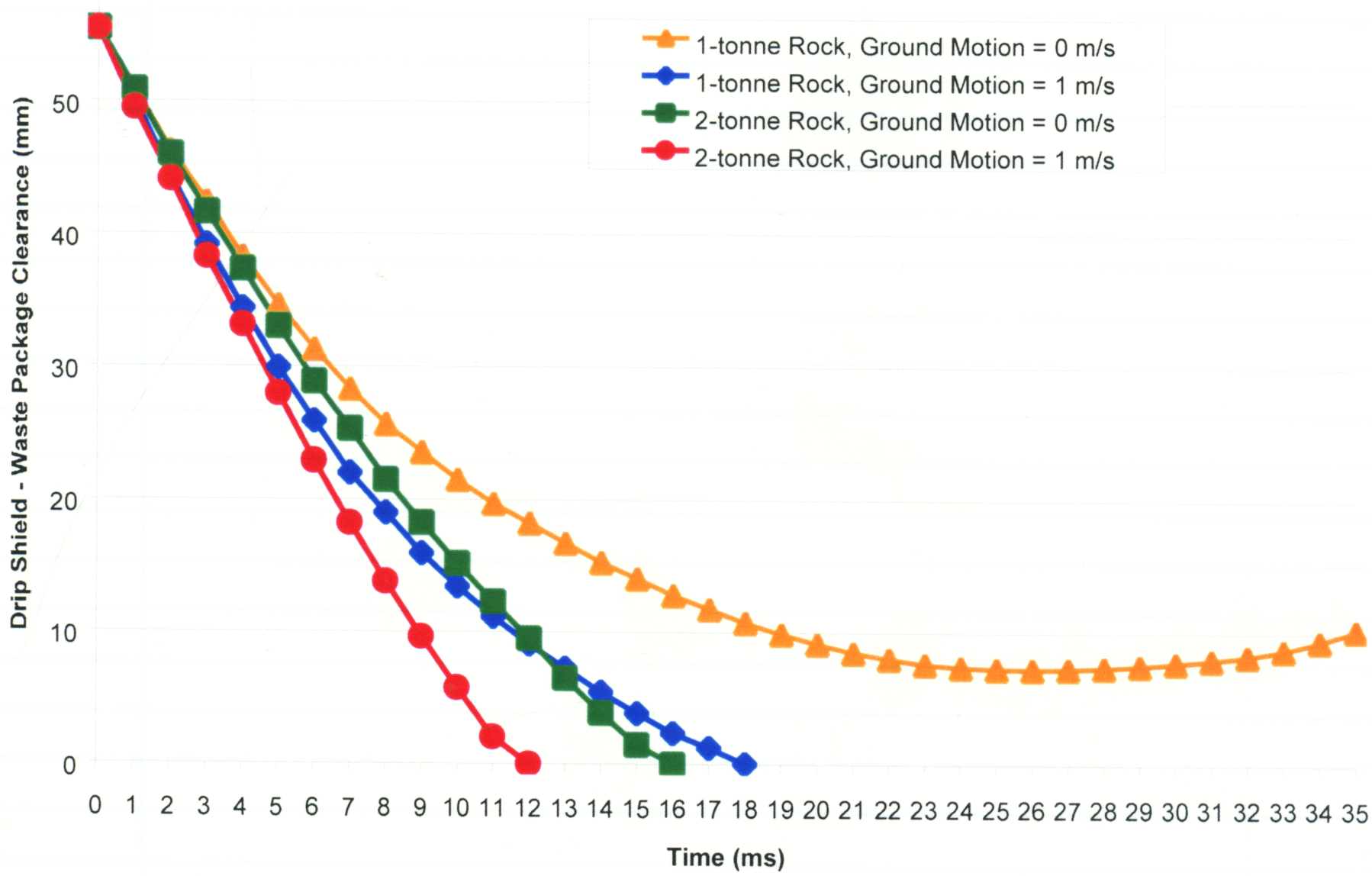

As can be seen from the plot on page 52, the 1-tonne rock block will drive the DS into the WP if ground motion is present. If ground motion is not present, then the rock block will significantly deform the DS but will not cause it to hit the WP. The 2-tonne rock block causes the DS to hit the WP regardless of whether ground motion is accounted for.

The DS will experience essentially the same deformation when it is driven into the WP regardless of the rock block size. Because the material response of the DS is not strain rate dependent, from a conservation of energy perspective, the DS is only capable of dissipating a fixed quantity of energy. Consequently, as the kinetic energy of the impact increases, the percentage of the total energy dissipated by the DS becomes smaller. As a result, the forces generated when the DS impacts the WP can be expected to increase proportionally.

The magnitude of stress generated in the DS after impacting the WP is illustrated in the figures on pages 54-56 of this notebook. It is interesting to note that the maximum Von Mises stress calculated corresponds to the 1-tonne rock block scenario (1 m/s ground motion). On review of the figure on page 54, it can be seen that the maximum Von Mises stress ~~correspond~~ occurs at an off-centered location, which is not the case for the 2-tonne rock block scenarios (see pages 55 & 56). The higher Von Mises stress for the 1-tonne rock block case can be attributed to the rock block rotating after the DS was driven into the WP and, therefore, causing greater deflections in the region of the highest stresses. This behavior was not seen for the 2-tonne rock block because the simulation terminates prematurely due to excessive deformation rate and wave speed ratios in the rock block elements located in the impact zone. These higher deformation rate and wave speed ratios are the result of the higher impact forces associated with the 2-tonne rock block.

DA 6/21/2000

Doug Tate 4/28/2000

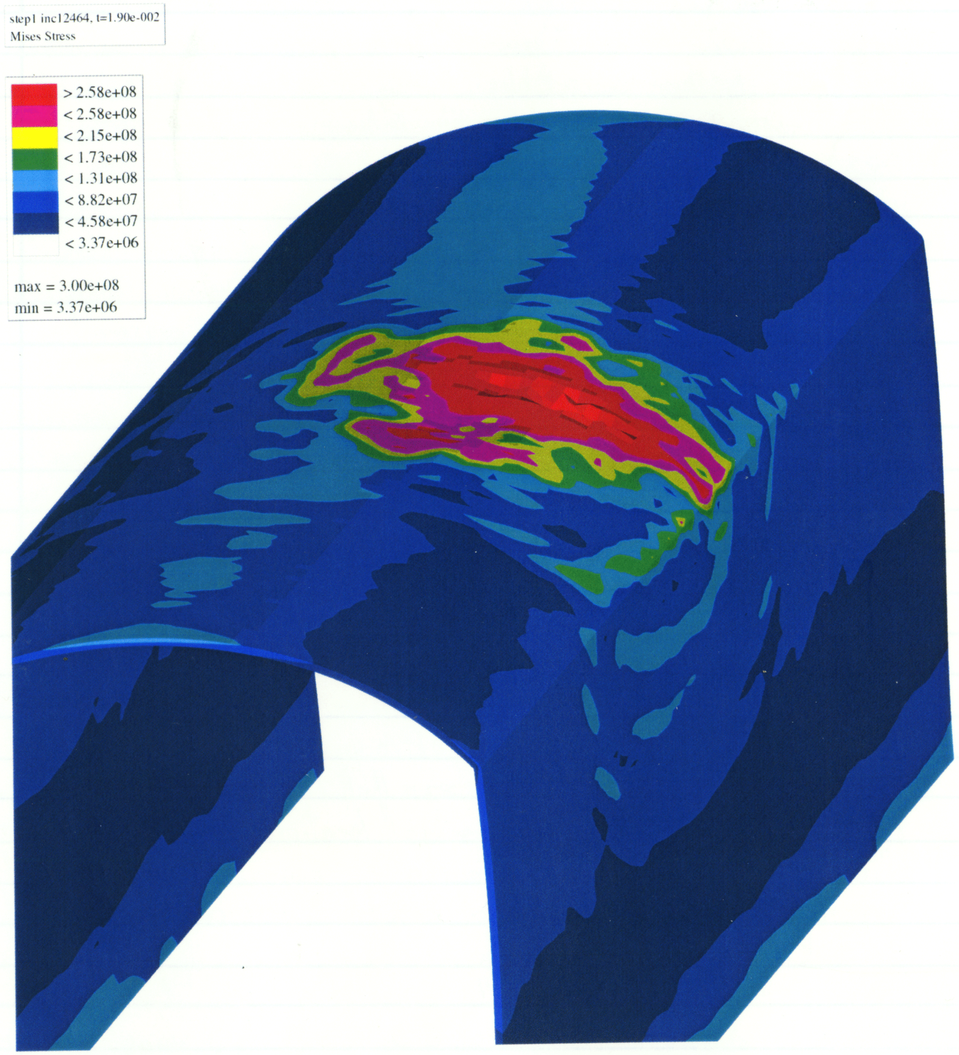

Von Mises stress (N/m^2) contour plot for the 1-tonne rock block, coarse mesh, and 1 m/s ground motion just before premature termination of the simulation. 6/21/2000

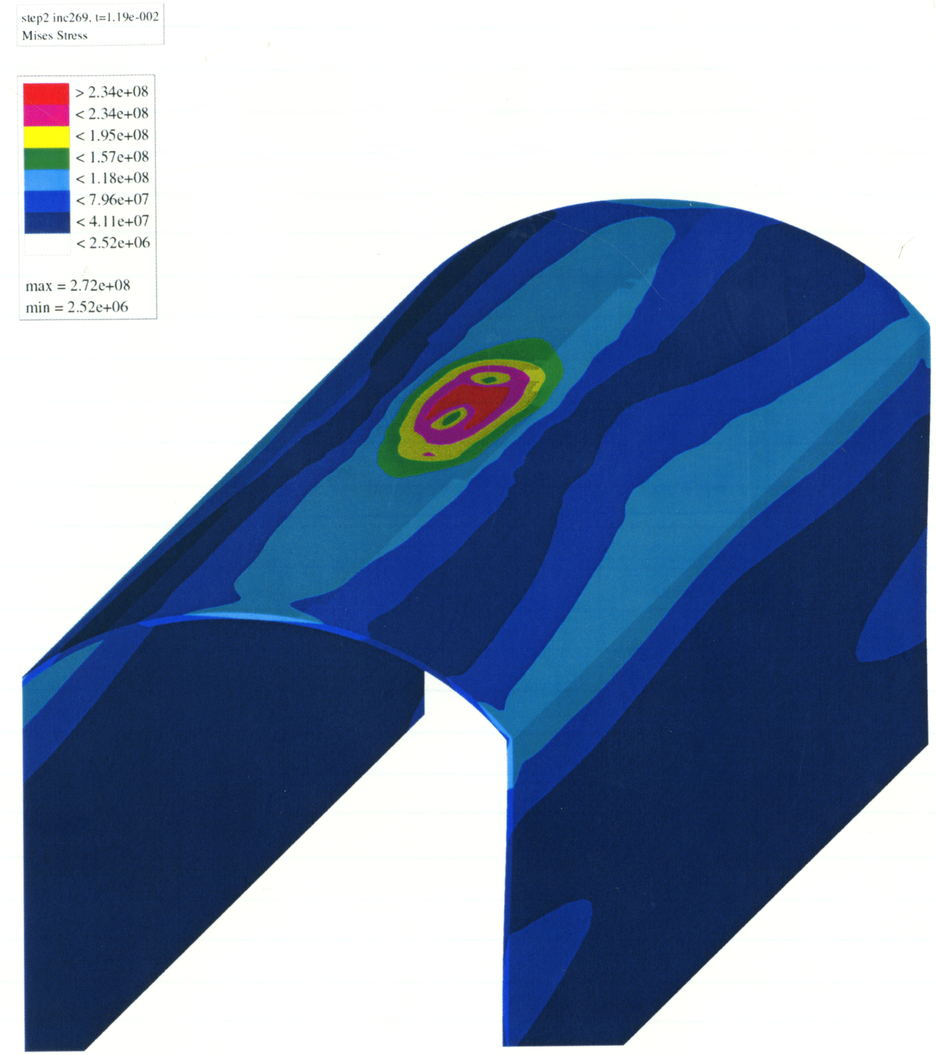

Von Mises stress (N/m^2) contour plot for the 2-tonne rock block, coarse mesh, and Ø m/s ground motion just before premature termination of the simulation.